

Novel fluconazole derivatives with promising antifungal activity

Nishad Thamban Chandrika,^{a,†} Sanjib K. Shrestha,^{a,†} Huy X. Ngo,^a Kaitlind C. Howard,^a and
Sylvie Garneau-Tsodikova^{a,*}

^a *University of Kentucky, Department of Pharmaceutical Sciences, Lexington, KY, 40536-0596, USA.*

[†] These authors contributed equally to this work.

* To whom the correspondence should be addressed: E-mail: [sylvie@tsodikova@uky.edu](mailto:sylvie@tsodikova.uky.edu); Tel: 859-218-1686.

The authors declare no conflict of interest.

Abstract

The fungistatic nature and toxicity concern associated with the azole drugs currently on the market have resulted in an increased demand for new azole antifungal agents for which these problematic characteristics do not exist. The extensive use of azoles has resulted in fungal strains capable of resisting the action of these drugs. Herein, we report the synthesis and antifungal activities of novel fluconazole (FLC) analogues with alkyl-, aryl-, cycloalkyl-, and dialkyl-amino substituents. We evaluated their antifungal activity by MIC determination and time-kill assay as well as their safety profile by hemolytic activity against murine erythrocytes as well as cytotoxicity against mammalian cells. The best compounds from our study exhibited broad-spectrum activity against most of the fungal strains tested, with excellent MIC values against a number of clinical isolates. The most promising compounds were found to be less hemolytic than the least hemolytic FDA-approved azole antifungal agent voriconazole (VOR). Finally, we demonstrated that the synthetic alkyl-amino FLC analogues displayed chain-dependent fungal membrane disruption as well as inhibition of ergosterol biosynthesis as possible mechanisms of action.

Keywords: Azoles, Clinical isolates, Cytotoxicity, Hemolysis, Time-kill studies.

1. Introduction

The rise in the number of infections caused by fungi poses a serious threat to human health and life.¹ Fungal infections can be endogenous (*e.g.*, *Candida* infections) or acquired from the environment (*e.g.*, *Cryptococcus* and *Aspergillus* infections). Invasive fungal infections have become a major problem for patients with immunodeficiency syndrome (*e.g.*, AIDS), organ transplant patients, and patients receiving chemotherapeutic agents for cancer treatment.²⁻⁴ Clinically, candidiasis, aspergillosis, and cryptococcosis are the major infections in immunocompromised patients.^{5,6} *Candida* and *Aspergillus* species are responsible for the majority of documented fungal infections. Recent studies indicated an epidemiological shift towards infections caused by emerging non-*albicans* *Candida* and *Aspergillus* species resistant to the current antifungal drugs.⁷⁻⁹ Non-*albicans* *Candida* species such as *C. glabrata*, *C. parapsilosis*, *C. tropicalis*, and *C. krusei* are more prominent now and they account for more incidence of invasive candidiasis such as candidemia than *C. albicans*.¹⁰⁻¹³ The relative presence of these fungal strains is region dependent. For example, *C. glabrata* is the second most common species after *C. albicans* in North America.¹⁴ Fungal strains such as *C. parapsilosis* and *C. tropicalis* are relatively more common in Europe, Australia, Latin America, and Asia.¹⁵⁻¹⁷ As resistance to the currently available antifungal agents is emerging in many of these non-*albicans* *Candida*, there is a need for developing novel antifungals.¹⁸

Most of the current drugs on the market are either highly toxic (*e.g.*, amphotericin B (AmB)) or becoming ineffective due to appearance of resistant fungal strains (*e.g.*, azoles such as fluconazole (FLC) and voriconazole (VOR)) (Fig. 1).¹⁹ Azoles are the most frequent class of antifungals used to treat fungal infections as they are inexpensive and are available for oral administration.²⁰ However, there is an extensive documentation of intrinsic and developed

resistance to azole drugs among *C. albicans* and non-*albicans Candida* species. As the frequency of occurrence of infections caused by non-*albicans Candida* species is increasing in clinical settings, there is currently a need to improve on the existing azole scaffolds to develop novel antifungals. Various studies were reported by our and other groups, which illustrated the role of alkylation on different drug scaffolds resulting in promising antifungal activity.²¹⁻²⁷ There are examples of 2,4-difluoro-2-(1*H*-1,2,4-triazolo-1-yl)acetophenone analogues with linear C₅-C₈ alkyl chains²⁵ and of an *n*-alkylated ebsulfur derivative with a linear C₅ alkyl chain, which displayed strong antifungal activity.²⁴ Similarly, examples of aminoglycosides (*e.g.*, kanamycin B (KANB) and tobramycin (TOB)) with linear alkyl chains with 12 and 14 carbons (C₁₂ and C₁₄) displaying antifungal activity were also reported.^{21, 22}

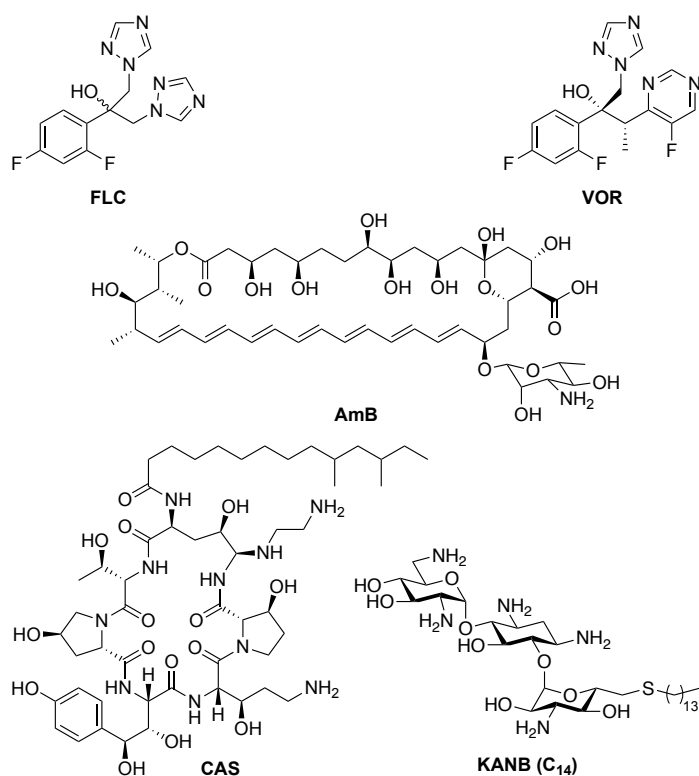


Fig. 1. Structures of all antifungal agents used as controls in this study.

Based on the information provided above and the promise shown by these small molecules, herein, we decided to generate novel FLC derivatives in which the triazole ring on the carbon alpha to the dihalophenyl ring of FLC was displaced by various linear alkyl-, aryl-, dialkyl-, and cycloalkyl-amino substituents. We report the synthesis of twelve novel FLC derivatives (Fig. 2) and their antifungal activity against a variety of *C. albicans*, non-*albicans Candida*, *Aspergillus*, and *Cryptococcus* strains as established by *in vitro* MIC determination as well as by time-kill studies. We explore the hemolytic activity as well as cytotoxicity of these compounds against murine erythrocytes and mammalian cell lines, respectively. Finally, we investigate the potential mechanism of action of selected compounds by probing their ability to disrupt fungal membrane.

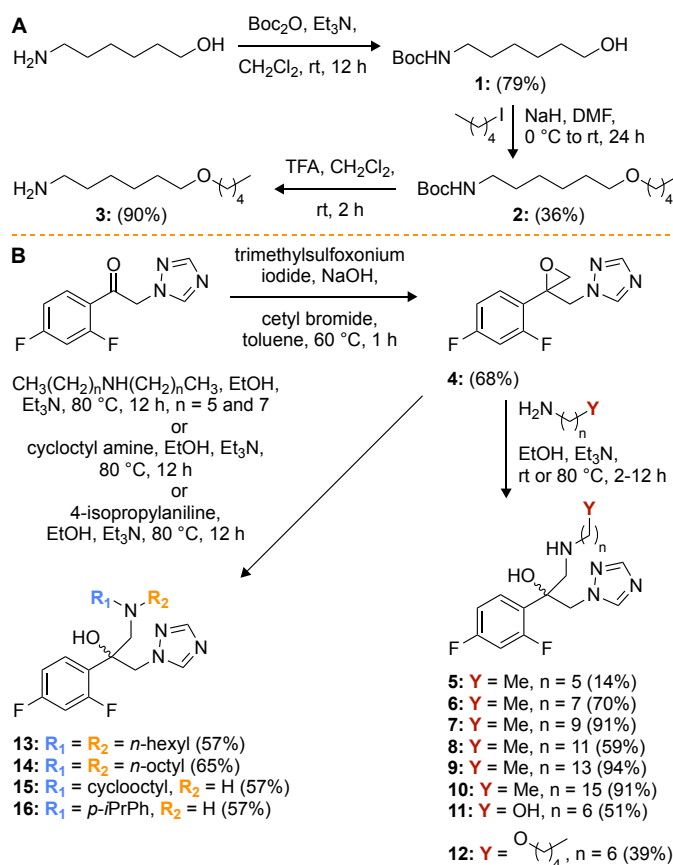


Fig. 2. Synthetic schemes for the preparation of **A.** amine derivative **3**, and **B.** novelazole analogues **5-16**.

2. Results and discussion

2.1. Design and synthesis of antifungal agents 5-16. We synthesized the alkyl-/aryl- and cycloalkyl-amino FLC derivatives **5-16** in two steps by using the commercially available fluorinated compound 2,4-difluoro-2-(1*H*-1,2,4-triazo-1-yl)acetophenone as a starting material (Fig. 2B). We first converted the carbonyl group of 2,4-difluoro-2-(1*H*-1,2,4-triazo-1-yl)acetophenone to an epoxide by using trimethylsulfoxonium iodide in the presence of a strong base and a surfactant to yield the oxirane intermediate **4**, which we then reacted with various amines (all commercially available, with the exception of amine **3** used in the synthesis of derivative **12**) under mild basic conditions to afford derivatives **5-16**. The amine **3** used for the synthesis of derivative **12** was prepared in three steps (Fig. 2A). The amino group of 6-aminohexanol was protected with Boc to yield compound **1**, which was then subjected to nucleophilic substitution reaction with 1-iodopentane. The deprotection of the Boc group of intermediate **2** yielded the desired amine **3**.

2.2. Antifungal activity and structure-activity-relationship (SAR) analysis. We first evaluated the antifungal activity of the newly prepared FLC derivatives **5-16** against a panel of seven *C. albicans* (ATCC 10231 (**A**), ATCC 64124(R) (**B**), ATCC MYA-2876(S) (**C**), ATCC 90819(R) (**D**), ATCC MYA-2310(S) (**E**), ATCC MYA-1237(R) (**F**), and ATCC MYA-1003(R) (**G**)), three non-*albicans Candida* (*C. glabrata* ATCC 2001 (**H**), *C. krusei* ATCC 6258 (**I**), and *C. parapsilosis* ATCC 22019 (**J**)), and three *Aspergillus* (*A. flavus* ATCC MYA-3631 (**K**), *A. nidulans* ATCC

38163 (**L**), and *A. terreus* ATCC MYA-3633 (**M**) strains using a concentration range of 0.03-31.3 µg/mL (Tables 1 and S1). We used the commercially available antifungal agents such as AmB, caspofungin (CAS), FLC, and VOR as positive controls for comparison. For derivatives **5-16** as well as the reference drugs AmB and CAS, we reported MIC-0 values, which correspond to no visible growth. We reported MIC-2 values (*i.e.*, 50% growth inhibition) for FLC and VOR against all fungal strains tested with the exception of strain **A** by VOR. We defined antifungal activity as excellent (0.03-1.95 µg/mL), good (3.9 µg/mL), moderate (7.8-15.6 µg/mL), or poor (\geq 31.3 µg/mL) based on MIC values. In this manuscript, we performed all activity comparisons by using the MIC values reported in µg/mL (*Note*: the corresponding MIC values are also provided in µM into parentheses in Tables 1, 2, S1, and S2).

Table 1: MIC values^a (in µg/mL) (the corresponding values in µM are provided in Table S1) determined for compounds **5-16** and for four control antifungal agents (AmB, CAS, FLC, and VOR) against various yeast strains and filamentous fungi. Each experiment was performed in triplicate.

Cpd #	Yeast strains										Filamentous fungi		
	A	B	C	D	E	F	G	H	I	J	K	L	M
5	7.8	>31.3	15.6	31.3	31.3	>31.3	31.3	15.6	7.8	0.975	>31.3	>31.3	>31.3
6	0.975	>31.3	31.3	7.8	31.3	15.6	31.3	7.8	0.975	0.06	>31.3	1.95	15.6
7	0.48	15.6	3.9	3.9	7.8	7.8	7.8	0.975	0.48	0.03	7.8	0.975	3.9
8	0.975	15.6	3.9	1.95	15.6	7.8	15.6	0.975	0.975	0.48	7.8	1.95	3.9
9	1.95	>31.3	>31.3	7.8	31.3	>31.3	31.3	0.975	3.9	0.48	>31.3	3.9	7.8
10	>31.3	>31.3	31.3	31.3	3.9-31.3	>31.3	>31.3	0.975	3.9	0.48	>31.3	3.9	>31.3
11	>31.3	>31.3	31.3	31.3	>31.3	>31.3	>31.3	>31.3	>31.3	>31.3	>31.3	>31.3	>31.3
12	3.9	>31.3	31.3	3.9	15.6	3.9	7.8	15.6	1.95	0.24	>31.3	7.8	31.3
13	>31.3	>31.3	>31.3	>31.3	>31.3	>31.3	>31.3	>31.3	>31.3	31.3	>31.3	>31.3	>31.3
14	31.3	>31.3	31.3	31.3	>31.3	31.3	>31.3	31.3	31.3	0.975	>31.3	15.6	>31.3
15	31.3	31.3	>31.3	31.3	3.9-31.3	31.3	>31.3	31.3	31.3	3.9	31.3	>31.3	>31.3
16	>31.3	>31.3	>31.3	31.3	31.3	31.3	31.3	7.8	>31.3	7.8	31.3	7.8	15.6
AmB	3.9	3.9	1.95	0.975	1.95	3.9	3.9	1.95	3.9	1.95	15.6	3.9	3.9
CAS	0.975	0.24	0.06	0.12	0.12	0.24	0.48	0.06	0.48	1.95	>31.3	>31.3	>31.3
FLC	62.5	>125	15.6	>125	>125	62.5	62.5	>31.3	>31.3	1.95	62.5	62.5	62.5
VOR	0.24	3.9	1.95	1.95	0.975	7.8	1.95	0.06	0.12	<0.03	0.24	0.12	0.12

Yeast strains: **A** = *Candida albicans* ATCC 10231, **B** = *C. albicans* ATCC 64124, **C** = *C. albicans* ATCC MYA-2876(S), **D** = *C. albicans* ATCC 90819(R), **E** = *C. albicans* ATCC MYA-2310(S), **F** = *C. albicans* ATCC MYA-1237(R), **G** = *C. albicans* ATCC MYA-1003(R), **H** = *Candida glabrata* ATCC 2001, **I** = *Candida krusei* ATCC 6258, **J** = *Candida parapsilosis* ATCC 22019. NOTE: Here, the (S) and (R) indicate that ATCC reports these strains to be susceptible (S) and resistant (R) to ITC and FLC.

Filamentous fungi: **K** = *Aspergillus flavus* ATCC MYA-3631, **L** = *Aspergillus nidulans* ATCC 38163, **M** = *Aspergillus terreus* ATCC MYA-3633.

Known antifungal agents: **AmB** = amphotericin B, **CAS** = caspofungin, **FLC** = fluconazole, **VOR** = voriconazole.

^a For yeast strains: MIC-0 values are reported for FLC analogues **5-16**, AmB, and CAS, whereas MIC-2 values are reported for azoles. For filamentous fungi, MIC-0 values are reported for all compounds.

By a survey of the data reported in Table 1, the following observations could rapidly be made. The introduction of a side-chain comprising (i) a terminal hydroxyl group as in compound **11**, (ii) a dialkyl-amino moiety as in derivatives **13** and **14**, (iii) a cycloalkyl-amino group as in compound **15**, and (iv) an aryl-amino functionality as in compound **16**, resulted in all cases in molecules that were generally poor antifungals. A few exceptions were noted: compounds **14** and **15** displayed excellent (0.975 $\mu\text{g/mL}$) and good (3.9 $\mu\text{g/mL}$) activity against the *C. parapsilosis* strain **J**. In contrary, we found that mono-alkylation resulted in much better antifungals. For derivatives **5-10**, we generally observed better activity against non-*albicans* *Candida* and *Aspergillus* strains than against *C. albicans*. More specifically, when exploring the data for strains **H-M**, we found that compounds **7** and **8** displayed excellent (0.03-1.95 $\mu\text{g/mL}$) activity against the non-*albicans* *Candida* strains **H**, **I**, and **J**, as well as against the *Aspergillus* strain **L**. Additionally, both compounds **7** and **8** exhibited moderate (7.8 $\mu\text{g/mL}$) and good (3.9 $\mu\text{g/mL}$) activity against the *Aspergillus* strains **K** and **M**, respectively. Compounds **5**, **6**, **9**, and **10**, displayed excellent activity (0.06-1.95 $\mu\text{g/mL}$) against strains **J**, (**I**, **J** and **L**), (**H** and **J**), and (**H** and **J**), respectively. Compounds **5**, **6**, and **9** displayed moderate activity (7.8-15.6 $\mu\text{g/mL}$) against strains (**H** and **I**), (**H** and **M**), and **M**, respectively. In addition, derivatives **9** and **10** showed good (3.9 $\mu\text{g/mL}$) activity against strains **I** and **L**. When assessing the data for the *C. albicans* strains **A-G**, we found that compounds **6-9** exhibited excellent activity (0.48-1.95 $\mu\text{g/mL}$) against strain **A**. We also observed that derivatives **7** and **8** generally displayed good to moderate (3.9-15.6 $\mu\text{g/mL}$) activity against strains **B-G**, with the exception of compound **8** displaying excellent (1.95 $\mu\text{g/mL}$) activity against strain **D**. In addition, compounds **7** and **8** displayed excellent to good antifungal activity against most strains tested and derivative **9** displayed strong activity against non-*albicans* *Candida* and *Aspergillus* strains. These data indicated that the optimal chain lengths for maximal antifungal

activity were C₁₀ and C₁₂, and the general trend for activity *versus* chain length was C₁₀ > C₁₂ > C₈ > C₁₄ > C₁₆ = C₆. Finally, we observed that replacing one of the carbon atom in the side-chain by an oxygen as in compound **12** was detrimental as its activity against all strains was generally lower (higher MIC values) than that of its counterpart **8**.

Having established that derivatives **5-16** displayed excellent antifungal activity against non-*albicans Candida* strains, we further evaluated these compounds against three clinical strains of *C. glabrata* (**CG1**, **CG2**, and **CG3**) and *C. parapsilosis* (**CP1**, **CP2**, and **CP3**), as well as three *Cryptococcus neoformans* (**CN1**, **CN2**, and **CN3**) clinical isolates (Table 2). The trends observed in Table 2 correlated perfectly to those described for the data presented in Table 1. Compounds **11** and **13** were inactive against all nine clinical isolates tested, whereas compounds **14-16** exhibited excellent to good (0.975-3.9 µg/mL) activity against *C. parapsilosis* **CP1**, **CP2**, and **CP3**. For derivatives **5-10**, we generally observed excellent activity against most *C. glabrata*, *C. parapsilosis*, and *C. neoformans* clinical isolates. More precisely, we found that compound **8** displayed excellent (0.06-1.95 µg/mL) activity against all clinical isolates tested. Compounds **7**, **9**, and **10** displayed excellent (0.03-1.95 µg/mL) activity against all isolates, with the exception of *C. glabrata* **CG3**. In addition, compound **6** displayed excellent (0.12-1.95 µg/mL) activity against **CG2**, **CP1**, **CP2**, **CP3**, and **CN1**, whereas compound **5** was found to display excellent (0.975 µg/mL) activity against *C. parapsilosis* **CP1**, **CP2**, and **CP3** isolates. Overall, compounds **6-10** displayed better activity against the clinical isolates presented in Table 2 than they did against the commercially available strains for which the data are presented in Table 1. In general, we found that the three most active compounds synthesized (based on the data from Tables 1 and 2), **7-9**, displayed better activity than FLC and similar or better activity than AmB against most of the fungal strains tested, as well as better activity than CAS against the three *Aspergillus* strains tested.

When examining the data obtained with clinical isolates of *C. glabrata*, *C. parapsilosis*, and *C. neoformans* (Table 2), we observed that compounds **7-9** displayed similar or better activity than both CAS and FLC. When comparing compounds **7-9** to VOR, we found them to display stronger activity against some of the clinical strains tested.

Table 2: MIC values^a (in µg/mL) (the corresponding values in µM are provided in Table S2) determined for compounds **5-16** and for two control antifungal agents (FLC and VOR) against various non-*albicans* *Candida* and *Cryptococcus neoformans* clinical isolates. Each experiment was performed in triplicate.

Cpd #	Yeast strains										
	H	CG1	CG2	CG3	J	CP1	CP2	CP3	CN1	CN2	CN3
5	7.8	31.3	7.8	31.3	0.975	0.975	0.975	0.975	7.8	>31.3	31.3
6	0.975	7.8	0.975	15.6	0.06	0.48	0.12	0.24	1.95	3.9	3.9
7	0.48	1.95	0.48	3.9	0.03	0.06	0.12	0.24	0.24	0.24	0.48
8	0.975	1.95	0.975	1.95	0.48	0.06	0.24	0.12	0.24	0.24	0.48
9	1.95	1.95	1.95	3.9	0.48	0.48	0.975	0.48	0.12	0.24	0.48
10	>31.3	1.95	0.975	7.8	0.48	0.975	0.48	0.975	0.48	0.48	0.48
11	>31.3	>31.3	>31.3	>31.3	>31.3	31.3	31.3	31.3	>31.3	>31.3	>31.3
12	3.9	15.6	1.95	31.3	0.24	0.12	0.12	0.12	0.48	1.95	1.95
13	>31.3	>31.3	>31.3	>31.3	31.3	>31.3	>31.3	>31.3	>31.3	>31.3	15.6
14	31.3	15.6	7.8	31.3	0.975	0.975	1.95	1.95	>31.3	>31.3	>31.3
15	31.3	31.3	15.6	31.3	3.9	0.975	0.975	1.95	7.8	>31.3	15.6
16	>31.3	7.8	7.8	7.8	7.8	3.9	3.9	3.9	7.8	31.3	>31.3
CAS	0.06	1.95	0.24	0.975	1.95	0.48	0.48	0.48	15.6	31.3	15.6
FLC	62.5	>31.3	>31.3	>31.3	1.95	0.975	0.975	0.975	7.8	>31.3	>31.3
VOR	0.24	0.975	3.9	>31.3	<0.03	<0.03	<0.03	<0.03	0.24	0.975	0.12

Yeast strains: H = *Candida glabrata* ATCC 2001, CG1-CG3 = *C. glabrata* clinical isolates, J = *Candida parapsilosis* ATCC 22019, CP1-CP3 = *C. parapsilosis* clinical isolates, CN1-CN3 = *Cryptococcus neoformans* clinical isolates.
Known antifungal agents: CAS = caspofungin, FLC = fluconazole, VOR = voriconazole.
^a For these yeast strains: MIC-0 values are reported for FLC analogues **5-16**, whereas MIC-2 values are reported for azoles.

The antifungals currently on the market are known to bind to proteins and be less efficient in intracellular matrices. For this reason, we tested the three best compounds, **7-9**, against three representative strains, the *C. albicans* **A**, the non-*albicans* *Candida* (*C. parapsilosis*) **J**, and the *Aspergillus* **L**, in presence and absence of fetal bovine serum (FBS) (Table 3). We found that the alkyl-amino azole analogue **7** retained its full antifungal activity (only 1 double dilution difference in some cases) against all three strains tested in the presence of FBS. Compound **8** retained its full activity against strain **J** and experienced a 2- and 4-fold decrease in activity in the presence of FBS against strains **A** and **L**, respectively. Compound **9** displayed a 2- to 8-fold decrease in activity

against the strains tested. Even though there was a small loss in activity in some instances, analogues **7-9** still remained good antifungal with the exception of compound **9** against strain **L**.

Table 3: MIC values^a (in µg/mL) determined for compounds **7-9** and for two control antifungal agents (AmB and VOR) against various yeast strains and filamentous fungi in the absence or presence of FBS. Each experiment was performed in triplicate.

Cpd #	Yeast strains				Filamentous fungi	
	<i>Candida albicans</i> ATCC 10231 (A) (no FBS)	<i>Candida albicans</i> ATCC 10231 (A) (+10% FBS)	<i>Candida parapsilosis</i> ATCC 22019 (J) (no FBS)	<i>Candida parapsilosis</i> ATCC 22019 (J) (+10% FBS)	<i>Aspergillus nidulans</i> ATCC 38163 (L) (no FBS)	<i>Aspergillus nidulans</i> ATCC 38163 (L) (+10% FBS)
7	0.48	0.48	0.03	0.06	0.975	1.95
8	0.975	1.95	0.48	0.24	1.95	7.8
9	1.95	7.8	0.48	0.975	3.9	31.2
AmB	3.9	7.8	1.95	15.6	3.9	15.6
VOR	0.48	0.48	0.015	0.015	0.12	0.12

2.3. Time-kill studies. The information regarding the rate and extend of fungicidal activity can be gathered by time-kill assays. To determine the fungistatic or fungicidal nature of the compounds generated, we performed time-kill assays over a 24-h period with one of the best FLC derivatives, compound **7**, and one of the good ones, compound **6**. These compounds and VOR (positive control) were tested against fungal strains *C. albicans* ATCC 10231 (**A**) and *C. parapsilosis* ATCC 22019 (**J**) (Fig. 3). At 4× their respective MIC values, when tested against strain **A**, compounds **6** and **7** were found to be fungistatic and to be better than the control drug VOR. When tested against strain **J**, both compounds also displayed fungistatic activity at up to 4× their MIC values. However, against strain **J**, compound **6** displayed lower reduction in fungal growth than VOR, but compound **7** displayed activity equal to VOR. Overall, the compounds **6** and **7** performed better in time-kill studies than the control drug VOR.

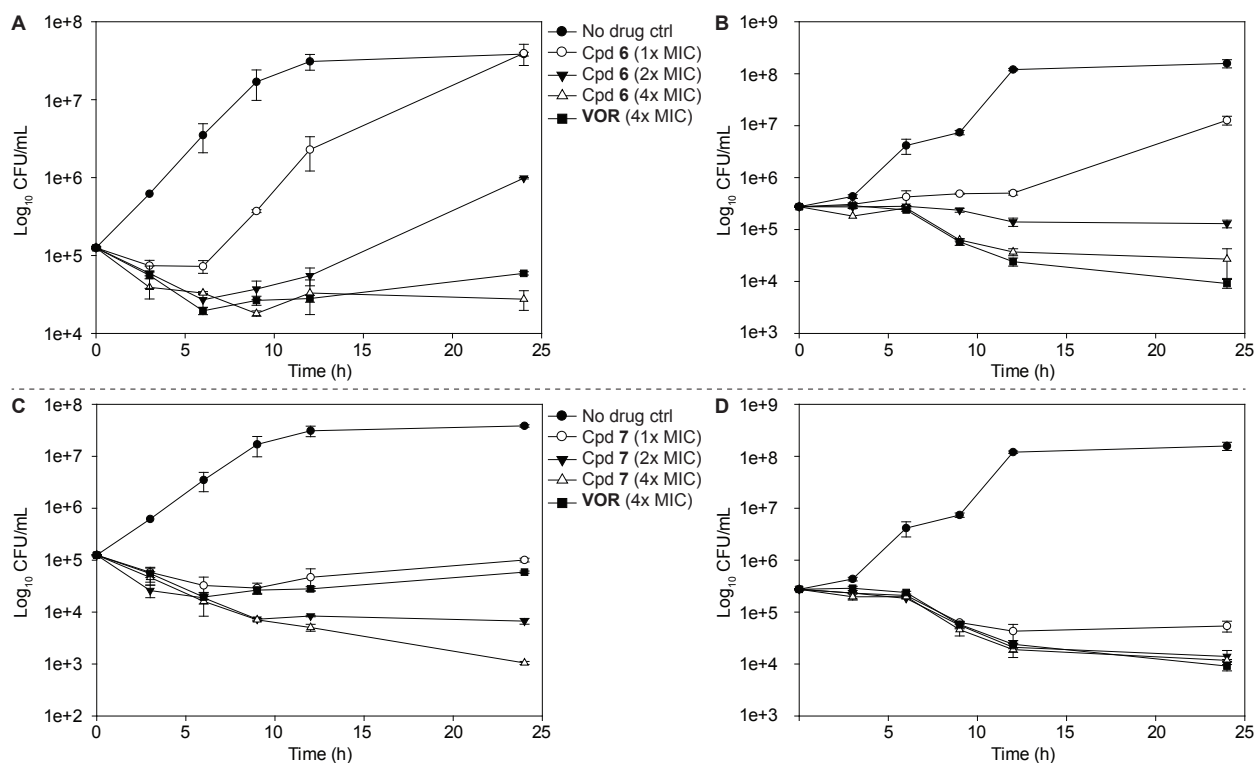


Fig. 3. Representative time-kill curves for compounds **6** and **7** against *C. albicans* ATCC 10231 (strain **A**; panels **A** and **C**, respectively) and *C. parapsilosis* ATCC 22019 (strain **J**; panels **B** and **D**, respectively). Fungal strains were treated with no drug (black circles), 1× MIC (white circles), 2× MIC (inverted black triangles), or 4× MIC (white triangles) of compounds **6** or **7**, or with 4× MIC (black squares) of VOR. The experiments were performed in duplicate.

2.4. Hemolysis assay. The promising antifungal activity shown by the synthetic analogues demanded further safety analysis for these compounds. We tested compounds **6-10** for their hemolytic activity against murine red blood cells (mRBCs) (Fig. 4 and Table S3). Compounds **6** (C_8) and **7** (C_{10}) displayed <10% and <40% hemolysis at concentrations of 31.3 $\mu\text{g/mL}$ (1- to 512-fold of its overall MIC values) and 15.6 $\mu\text{g/mL}$ (1- to 512-fold of its overall MIC values),

respectively. Similarly, compound **8** (C₁₂) induced only 21% lysis at 7.8 µg/mL (1- to 218-fold of its overall MIC values). In addition, compounds **9** (C₁₄) and **10** (C₁₆) displayed <50% and <10% hemolysis at concentrations of 31.3 µg/mL (1- to 256-fold of its overall MIC values) and 62.5 µg/mL (2- to 128-fold of its overall MIC values), respectively. By comparing the hemolysis of compounds **6-10** with their corresponding MIC values against the non-*albicans* *Candida*, *A. nidulans*, and *C. neoformans* strains tested, we concluded that all of these compounds displayed minimal hemolytic activity. Overall, compounds **6** and **10** displayed the lowest hemolytic activity. Importantly, some of the newly synthesized compounds displayed less hemolytic effect than the FDA-approved control drug VOR.

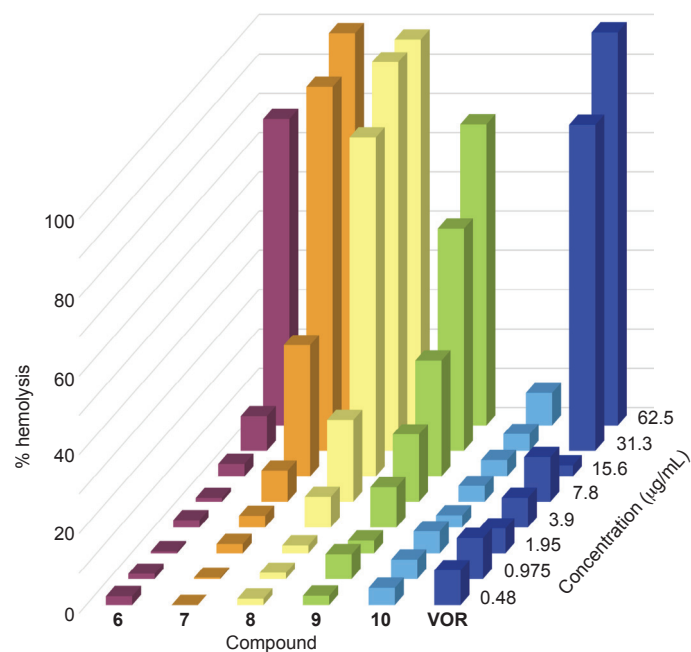


Fig. 4. 3D bar graph depicting the dose-dependent hemolytic activity of azole derivatives **6-10** and VOR against mRBCs, which were treated and incubated for 1 h at 37 °C with each compound

tested at concentrations ranging from 0.48-62.5 $\mu\text{g}/\text{mL}$. Triton X-100® (1% v/v) was used as a positive control (100% hemolysis, not shown).

2.5. *In vitro* cytotoxicity assay. Another crucial parameter to consider when developing antifungal drugs is their selectivity for fungal over mammalian cells. We tested our active compounds **6-10** against three different cell lines, HEK-293, BEAS-2B, and A549, along with the FDA-approved antifungal agent VOR as a positive control (Fig. 5). Against HEK-293, compounds **6**, **7**, and **10** exhibited no toxicity up to 31 $\mu\text{g}/\text{mL}$ (1- to 512-fold of its overall MIC values), 7.8 $\mu\text{g}/\text{mL}$ (1- to 256-fold of its overall MIC values), and 7.8 $\mu\text{g}/\text{mL}$ (1- to 16-fold of its overall MIC values), respectively. However, compounds **8** and **9** exhibited some toxicity (>50% cell survival) at a concentration of 3.9 $\mu\text{g}/\text{mL}$ (1- to 64-fold of its overall MIC values) against HEK-293. Interestingly, compounds **8-10** were non-toxic to both BEAS-2B and A549 at up to 7.8 $\mu\text{g}/\text{mL}$ (1- to 128-fold of its overall MIC values). In the case of compound **6**, no toxicity was observed against BEAS-2B (at 31 $\mu\text{g}/\text{mL}$) (1- to 512-fold of its overall MIC values) and A549 (at 15.5 $\mu\text{g}/\text{mL}$) (1- to 256-fold of its overall MIC values). With compound **10** we basically observed no toxicity against BEAS-2B and A549 at 7.8 $\mu\text{g}/\text{mL}$ (1- to 16-fold of its overall MIC values). A general trend of greater toxicity with respect to longer chain substitution was observed against the three cell lines. Compounds **6** and **7** exhibited better overall safety profiles than compounds **8-10**. When considering the very low MIC values for these analogues against clinical isolates, these cytotoxicity data provide us with a reasonable therapeutic window.

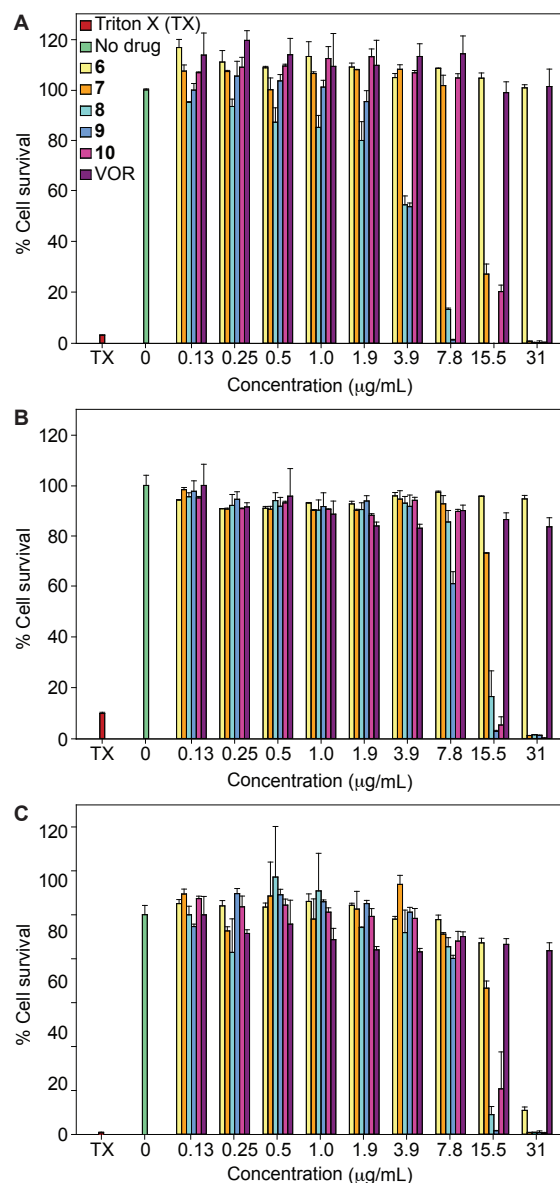


Fig. 5. Representative cytotoxicity assays of compounds **6-10** against three mammalian cell lines: **A.** HEK-293, **B.** BEAS-2B, and **C.** A549. Cells were treated with various concentrations of compounds **6** (yellow), **7** (orange), **8** (turquoise), **9** (blue), **10** (pink), and VOR (purple). The positive control consisted of cells treated with Triton X-100[®] (TX, 20% *v/v*, pink). The negative control consisted of cells treated with DMSO (no drug, green). The experiments were performed in duplicate.

2.6. Membrane permeabilization assay. Some amphiphilic molecules have been shown to cause membrane disruption and fungal cell death. Therefore, we decided to study the potential effect of compounds **8** and **9** with C₁₂ and C₁₄ linear alkyl chains to determine the impact of chain length on membrane disruption (Fig. 6). The control drug VOR and the KANB (C₁₄) derivative with a 14-carbon linear alkyl chain, were used as negative and positive controls, respectively. The propidium iodide (PI) dye was used as a probe as it can only enter cells with compromised membrane and bind to nucleic acid to emit fluorescence, which can be observed under a fluorescence microscope. At 4× MIC, the positive control KANB (C₁₄) significantly increased PI dye uptake by *C. albicans* ATCC 10231 (strain **A**), whereas the negative control VOR (at 4× MIC) did not allow for PI uptake by fungal cells. Compound **8** with a C₁₂ linear alkyl chain (at 4× MIC) induced cellular uptake of PI dye into *C. albicans* ATCC 10231 (strain **A**), whereas compound **9** (with a C₁₄ linear alkyl chain) did not cause cell membrane disruption. Interestingly, the chain length played a crucial role on membrane disruption of *C. albicans* ATCC 10231 (strain **A**), surprisingly with C₁₂ being more membrane disrupting than C₁₄. In order to completely understand the effect of chain length on membrane disruption, we additionally performed membrane permeabilization with compounds **5**, **6**, and **7** (C₆-C₁₀ linear alkyl chains) at 4× MIC. None of these compounds induced cellular uptake of the PI drug. From this study, we can conclude that one of the possible mechanisms of action for compound **8** is membrane disruption. Interestingly, any other linear chains beside the C₁₂ displayed no membrane disruption.

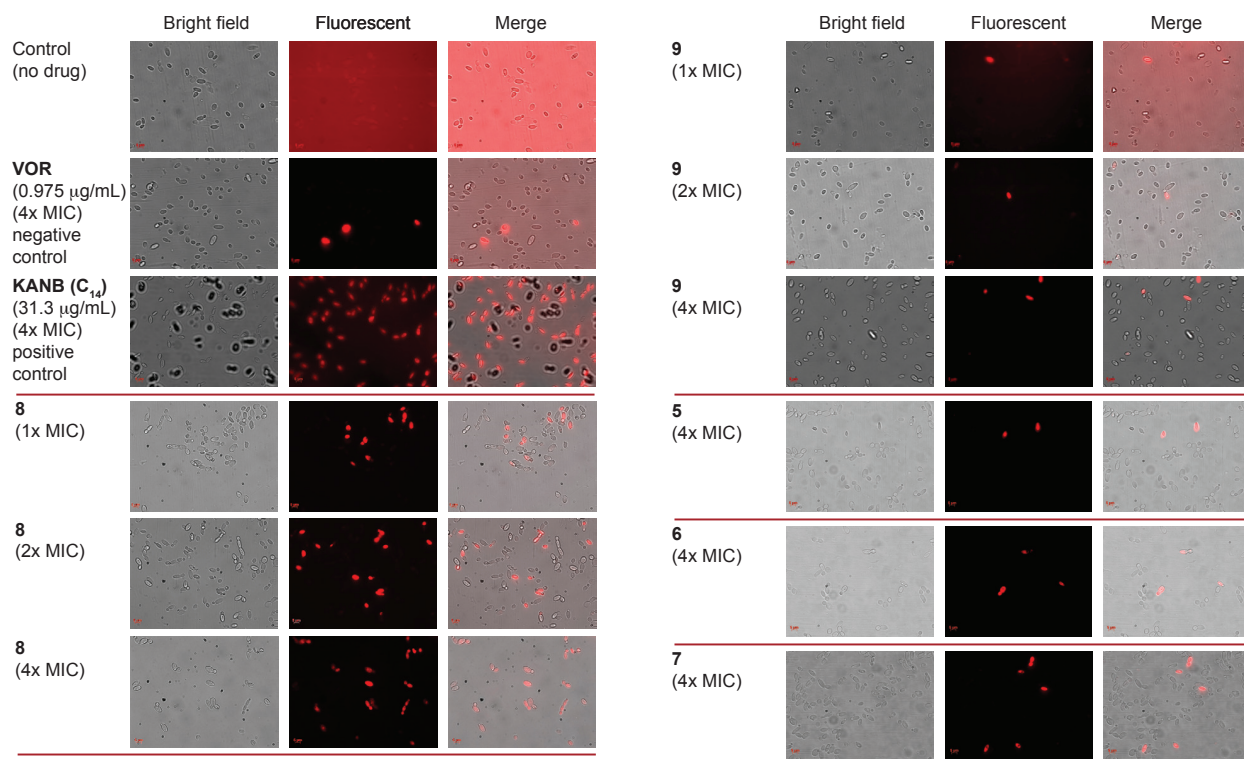
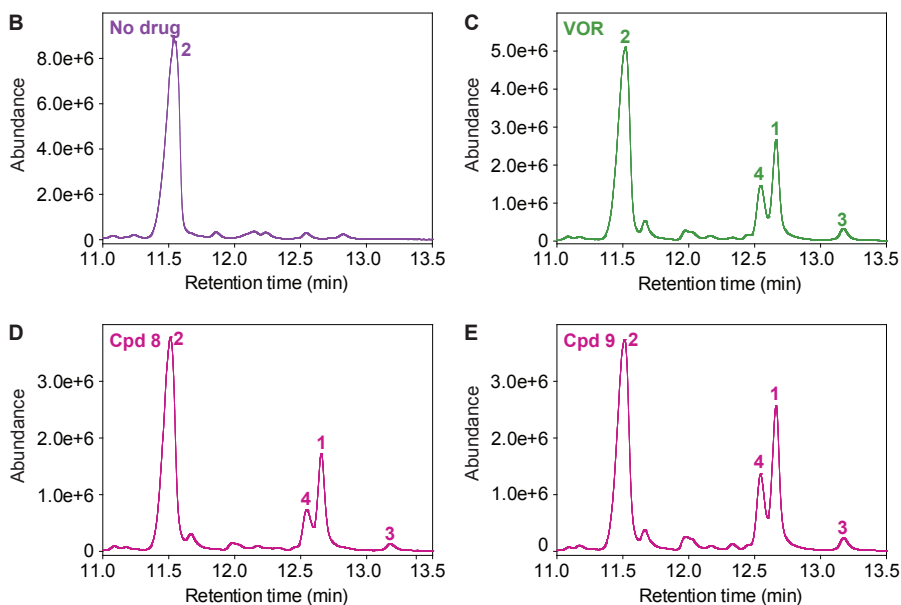
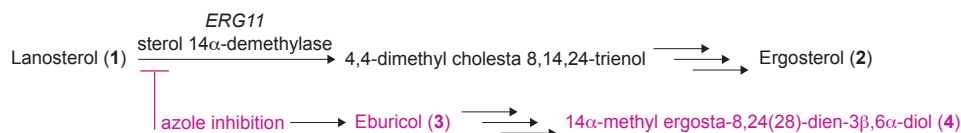


Fig. 6. Effect of the controls VOR (negative) and KANB (C_{14}) (positive) as well as compounds **5-9** on the cell membrane integrity of *C. albicans* ATCC 10231 (strain **A**). For the three columns on the left from top to bottom: Propidium iodide (PI) dye uptake by yeast cells without drug, with VOR ($0.975 \mu\text{g/mL}$), KANB (C_{14}) ($31.3 \mu\text{g/mL}$), and compound **8** ($1\times$, $2\times$, and $4\times$ MIC). For the three columns on the right from top to bottom: Propidium iodide (PI) dye uptake by yeast cells with compound **9** ($1\times$, $2\times$, and $4\times$ MIC), as well as compound **5**, **6**, and **7** at $4\times$ MIC. The experiments were performed in duplicate.

2.7. Sterol profile by GC-MS. Since out of our compounds displaying antifungal activity only compound **8** caused membrane disruption of *C. albicans* ATCC 10231 (strain **A**) in the membrane permeabilization assay (section 2.6), we decided to explore by using gas chromatography-mass

spectrometry (GC-MS) the effect of compounds **8** and **9** on sterol composition during ergosterol biosynthesis (the mechanism of action of other conventional azoles) (Fig. 7). We evaluated the effect of the compounds **8** and **9** on sterol composition in *C. albicans* ATCC 10231 (strain **A**) at sub-MIC levels of 0.48 µg/mL (Fig. 7D) and 0.975 µg/mL (Fig. 7E), respectively. We also used VOR at 0.12 µg/mL and no drug control for comparison (Fig. 7B and 7A, respectively). In the absence of drug, strain **A** accumulated 100% ergosterol (**2**), suggesting that the sterol biosynthesis was fully functional in this fungal strain. When treating strain **A** with VOR, we detected a lower amount of ergosterol (**2**, 50.80%), and an increased amount of lanosterol (**1**, 15.21%) and eburicol (**3**, 1.73%). However, when strain **A** was treated with compound **8**, we observed a relatively low amount of ergosterol (**2**, 36.62%) compared to VOR, but observed lower amounts of lanosterol (**1**, 10.03%), eburicol (**3**, 0.57%), and the fungistatic metabolite 14 α -methyl ergosta-8,24(28)-diene-3 β ,6 α -diol (**4**, 4.69%) with respect to VOR. Interestingly, when strain **A** was treated with compound **9**, we observed similar reduction in the amount of ergosterol (**2**, 36.43%) along with a related increase in lanosterol (**1**, 15.56%), eburicol (**3**, 1.16%) and the fungistatic metabolite 14 α -methyl ergosta-8,24(28)-diene-3 β ,6 α -diol (**4**, 15.56%). From these experiments, we can conclude that our compounds inhibit ergosterol biosynthesis similarly to the azole drug control VOR.

A. Simplified ergosterol biosynthetic pathway and products resulting from inhibition of *ERG11*:



F. Sterol composition of untreated and VOR-, cpd 8-, and cpd 9-treated *C. albicans* ATCC 10231 (strain A):

Sterol	Sterol composition (%)			
	No drug	VOR	Cpd 8	Cpd 9
Lanosterol (1)	ND	15.21	10.03	15.56
Ergosterol (2)	100.00	50.80	36.62	36.43
Eburicol (3)	ND	1.73	0.57	1.16
14 α -methyl ergosta-8,24(28)-dien-3 β ,6 α -diol (4)	ND	9.86	4.69	8.33

ND = not detected

Fig. 7. A. A simplified ergosterol biosynthetic pathway and products resulting from inhibition of *ERG11*. **B-E.** GC-MS chromatograms of the sterols extracted from untreated and antifungal-treated *C. albicans* ATCC 10231 (strain A). The fungal strain treated with DMSO (no drug control, panel B), VOR at 0.12 $\mu\text{g}/\text{mL}$ (panel C), compound 8 at 0.48 $\mu\text{g}/\text{mL}$ (panel D), and compound 9 at 0.975 $\mu\text{g}/\text{mL}$ (panel E). The peaks in these chromatograms are for lanosterol (1), ergosterol (2), eburicol (3), 14 α -methyl ergosta-8,24(28)-dien-3 β ,6 α -diol (4). **F.** A table summarizing the percentage of each sterol from panels B-E.

3. Conclusions

In summary, we have synthesized novel FLC derivatives in which the triazole ring on the carbon alpha to the dihalophenyl ring of FLC was displaced by various linear alkyl-, aryl-, dialkyl-, and cycloalkyl-amino substituents. We did not detect any antifungal activity with the aryl- and cycloalkyl-amino substituted FLC analogues. We observed that the antifungal activity of the alkyl-amino FLC derivatives depends on the length of the alkyl chains. Compounds **6-9** were identified as promising antifungal agents with low hemolytic activity and low cytotoxicity. These analogues displayed great activity against some of the *C. albicans*, non-*albicans Candida*, and *Aspergillus* strains, and, in addition they were particularly excellent against the clinical strains of *C. glabrata*, *C. parapsilosis*, as well as *C. neoformans* tested. These compounds also exhibited superior activity against the clinical strains when compared to the control drugs CAS, FLC, and VOR. The possible mechanism of action for these FLC analogues was identified as membrane disruption with compound **8** with a C₁₂ alkyl chain being more membrane disrupting than compound **9** with a C₁₄ alkyl chain. Additionally, they were found to inhibit ergosterol biosynthesis. In the future, outside of the scope of this work, it will be interesting to see how these promising molecules will fair in the drug development process.

Acknowledgments

This work was supported by startup funds from the University of Kentucky (to S.G.-T.) and by NIH grant AI090048 (to S.G.-T.). H.X.N. was in part supported by a Pharmaceutical Sciences Excellence in Graduate Achievement Fellowship from the College of Pharmacy at the University of Kentucky.

Author Contributions

N.T.C., S.K.S, and S.G.-T. design the study, analyzed the data, wrote the manuscript and supporting information, and made figures. N.T.C. and K.C.H. synthesized all compounds used in this study. H.X.N. performed the cytotoxicity assays and time-kill studies and generated Figs. 2 and 4. S.K.S. performed all other biochemical/biological experiments. N.T.C., S.K.S., H.X.N., and S.G.-T. reviewed the manuscript and supporting information. All authors approved the manuscript and supporting information.

Supporting Information Available: The supporting information includes experimental procedures for the chemistry and biological work performed. More specifically, it includes: (i) materials and instrumentation, (ii) protocols for the synthesis of compounds **1-16**, (iii) a list of antifungal agents used, (iv) a list of organisms against which compounds **5-16** were tested along with their culture conditions, and experimental procedures for (v) MIC value determination, (vi) time-kill studies, (vii) hemolytic activity, (viii) *in vitro* cytotoxicity assay, (xi) membrane permeabilization assay, and (x) sterol profile by GC-MS. ¹H and ¹³C NMR spectra (Fig. S1-S32) of all compounds generated in this study are also presented. The MIC values in μM are provided in Tables S1 and S2. The exact percentages with SDEV that were used to prepare Fig. 4 are provided in Table S3.

Corresponding Author Information

Abbreviations

AmB, amphotericin B; ATCC, American Type Culture Collection; CAS, caspofungin; CLSI, Clinical and Laboratory Standards Institute; FBS, fetal bovine serum; FLC, fluconazole; KANB, kanamycin B; mRBCs, murine red blood cells; PI, propidium iodide; SAR, structure-activity-relationship; TOB, tobramycin; VOR, voriconazole.

References

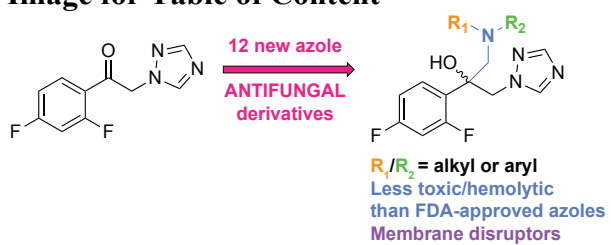
1. Garibotto, F. M.; Garro, A. D.; Masman, M. F.; Rodriguez, A. M.; Luiten, P. G.; Raimondi, M.; Zacchino, S. A.; Somlai, C.; Penke, B.; Enriz, R. D. New small-size peptides possessing antifungal activity. *Bioorg. Med. Chem.* **2010**, 18, 158-167.
2. Beck-Sague, C.; Jarvis, W. R. Secular trends in the epidemiology of nosocomial fungal infections in the United States, 1980-1990. National Nosocomial Infections Surveillance System. *J. Infect. Dis.* **1993**, 167, 1247-1251.
3. Pfaller, M. A.; Diekema, D. J. Epidemiology of invasive candidiasis: a persistent public health problem. *Clin. Microbiol. Rev.* **2007**, 20, 133-163.
4. Pannuti, C.; Gingrich, R.; Pfaller, M. A.; Kao, C.; Wenzel, R. P. Nosocomial pneumonia in patients having bone marrow transplant. Attributable mortality and risk factors. *Cancer* **1992**, 69, 2653-2662.
5. Latge, J. P. *Aspergillus fumigatus* and aspergillosis. *Clin. Microbiol. Rev.* **1999**, 12, 310-350.

6. Steenbergen, J. N.; Casadevall, A. Prevalence of *Cryptococcus neoformans* var. *neoformans* (Serotype D) and *Cryptococcus neoformans* var. *grubii* (Serotype A) isolates in New York City. *J. Clin. Microbiol.* **2000**, 38, 1974-1976.
7. Groll, A. H.; Walsh, T. J. Uncommon opportunistic fungi: new nosocomial threats. *Clin. Microbiol. Infect.* **2001**, 7 Suppl 2, 8-24.
8. Wald, A.; Leisenring, W.; van Burik, J. A.; Bowden, R. A. Epidemiology of *Aspergillus* infections in a large cohort of patients undergoing bone marrow transplantation. *J. Infect. Dis.* **1997**, 175, 1459-1466.
9. Viscoli, C.; Girmenia, C.; Marinus, A.; Collette, L.; Martino, P.; Vandercam, B.; Doyen, C.; Lebeau, B.; Spence, D.; Krcmery, V.; De Pauw, B.; Meunier, F. Candidemia in cancer patients: a prospective, multicenter surveillance study by the Invasive Fungal Infection Group (IFIG) of the European Organization for Research and Treatment of Cancer (EORTC). *Clin. Infect. Dis.* **1999**, 28, 1071-1079.
10. Miceli, M. H.; Diaz, J. A.; Lee, S. A. Emerging opportunistic yeast infections. *Lancet Infect. Dis.* **2011**, 11, 142-151.
11. Pfaller, M. A.; Diekema, D. J.; Gibbs, D. L.; Newell, V. A.; Ellis, D.; Tullio, V.; Rodloff, A.; Fu, W.; Ling, T. A.; Global Antifungal Surveillance, G. Results from the ARTEMIS DISK Global Antifungal Surveillance Study, 1997 to 2007: a 10.5-year analysis of susceptibilities of *Candida* Species to fluconazole and voriconazole as determined by CLSI standardized disk diffusion. *J. Clin. Microbiol.* **2010**, 48, 1366-1377.
12. Puig-Asensio, M.; Peman, J.; Zaragoza, R.; Garnacho-Montero, J.; Martin-Mazuelos, E.; Cuenca-Estrella, M.; Almirante, B.; Prospective Population Study on Candidemia in Spain, P.; Hospital Infection Study, G.; Medical Mycology Study Group of the Spanish Society of Infectious, D.; Clinical, M.; Spanish Network for Research in Infectious, D. Impact of therapeutic strategies on the prognosis of candidemia in the ICU. *Crit. Care Med.* **2014**, 42, 1423-1432.
13. Guo, F.; Yang, Y.; Kang, Y.; Zang, B.; Cui, W.; Qin, B.; Qin, Y.; Fang, Q.; Qin, T.; Jiang, D.; Li, W.; Gu, Q.; Zhao, H.; Liu, D.; Guan, X.; Li, J.; Ma, X.; Yu, K.; Chan, D.; Yan, J.; Tang, Y.; Liu, W.; Li, R.; Qiu, H.; China, S. T. Invasive candidiasis in intensive care units in China: a multicentre prospective observational study. *J. Antimicrob. Chemother.* **2013**, 68, 1660-1668.

14. Pfaller, M. A.; Diekema, D. J. Epidemiology of invasive mycoses in North America. *Crit. Rev. Microbiol.* **2010**, *36*, 1-53.
15. Chen, S.; Slavin, M.; Nguyen, Q.; Marriott, D.; Playford, E. G.; Ellis, D.; Sorrell, T.; Australian Candidemia, S. Active surveillance for candidemia, Australia. *Emerg. Infect. Dis.* **2006**, *12*, 1508-1516.
16. Wang, H.; Xiao, M.; Chen, S. C.; Kong, F.; Sun, Z. Y.; Liao, K.; Lu, J.; Shao, H. F.; Yan, Y.; Fan, H.; Hu, Z. D.; Chu, Y. Z.; Hu, T. S.; Ni, Y. X.; Zou, G. L.; Xu, Y. C. *In vitro* susceptibilities of yeast species to fluconazole and voriconazole as determined by the 2010 National China Hospital Invasive Fungal Surveillance Net (CHIF-NET) study. *J. Clin. Microbiol.* **2012**, *50*, 3952-3959.
17. Nucci, M.; Queiroz-Telles, F.; Tobon, A. M.; Restrepo, A.; Colombo, A. L. Epidemiology of opportunistic fungal infections in Latin America. *Clin. Infect. Dis.* **2010**, *51*, 561-570.
18. Xiao, M.; Fan, X.; Chen, S. C.; Wang, H.; Sun, Z. Y.; Liao, K.; Chen, S. L.; Yan, Y.; Kang, M.; Hu, Z. D.; Chu, Y. Z.; Hu, T. S.; Ni, Y. X.; Zou, G. L.; Kong, F.; Xu, Y. C. Antifungal susceptibilities of *Candida glabrata* species complex, *Candida krusei*, *Candida parapsilosis* species complex and *Candida tropicalis* causing invasive candidiasis in China: 3 year national surveillance. *J. Antimicrob. Chemother.* **2015**, *70*, 802-810.
19. Pore, V. S.; Aher, N. G.; Kumar, M.; Shukla, P. K. Design and synthesis of fluconazole/bile acid conjugate using click reaction. *Tetrahedron* **2006**, *62*, 11178-11186.
20. Whaley, S. G.; Berkow, E. L.; Rybak, J. M.; Nishimoto, A. T.; Barker, K. S.; Rogers, P. D. Azole antifungal resistance in *Candida albicans* and emerging non-*albicans* *Candida* species. *Front. Microbiol.* **2016**, *7*, 2173.
21. Shrestha, S. K.; Fosso, M. Y.; Green, K. D.; Garneau-Tsodikova, S. Amphiphilic tobramycin analogues as antibacterial and antifungal agents. *Antimicrob. Agents Chemother.* **2015**, *59*, 4861-4869.
22. Fosso, M. Y.; Shrestha, S. K.; Green, K. D.; Garneau-Tsodikova, S. Synthesis and bioactivities of kanamycin B-derived cationic amphiphiles. *J. Med. Chem.* **2015**, *58*, 9124-9132.
23. Thamban Chandrika, N.; Shrestha, S. K.; Ngo, H. X.; Garneau-Tsodikova, S. Synthesis and investigation of novel benzimidazole derivatives as antifungal agents. *Bioorg. Med. Chem.* **2016**, *24*, 3680-3686.

24. Ngo, H. X.; Shrestha, S. K.; Garneau-Tsodikova, S. Identification of ebsulfur analogues with broad-spectrum antifungal activity. *ChemMedChem* **2016**, *11*, 1507-1516.
25. Shrestha, S. K.; Garzan, A.; Garneau-Tsodikova, S. Novel alkylated azoles as potent antifungals. *Eur. J. Med. Chem.* **2017**, *133*, 309-318.
26. Chang, C. W.; Fosso, M.; Kawasaki, Y.; Shrestha, S.; Bensaci, M. F.; Wang, J.; Evans, C. K.; Takemoto, J. Y. Antibacterial to antifungal conversion of neamine aminoglycosides through alkyl modification. Strategy for reviving old drugs into agrofungicides. *J. Antibiot.* **2010**, *63*, 667-672.
27. Shrestha, S.; Grilley, M.; Fosso, M. Y.; Chang, C. W.; Takemoto, J. Y. Membrane lipid-modulated mechanism of action and non-cytotoxicity of novel fungicide aminoglycoside FG08. *PLoS One* **2013**, *8*, e73843.

Image for Table of Content



Supporting Information

Novel fluconazole derivatives with promising antifungal activity

Nishad Thamban Chandrika,^{a,†} Sanjib K. Shrestha,^{a,†} Huy. X. Ngo,^a Kaitlind C. Howard,^a and
Sylvie Garneau-Tsodikova^a

^a Department of Pharmaceutical Sciences, University of Kentucky, Lexington, KY, 40536-0596, USA.

[†] These authors contributed equally to this work.

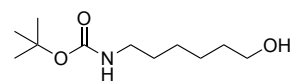
Table of content:	Page #
1. Chemistry:	
1.1. Materials and instrumentation	S1-S2
1.2. Experimental protocols for the preparation of compounds 1-16	S2-S9
2. Biological studies:	
2.1. Antifungal agents	S9-S10
2.2. Organisms and culture conditions	S10
2.3. MIC value determination by <i>in vitro</i> antifungal assay	S10-S11
Table S1	S12
Table S2	S12
2.4. Time-kill studies	S12-S13
2.5. Hemolytic activity assay	S13
Table S3	S14
2.6. <i>In vitro</i> cytotoxicity assay	S14
2.7. Membrane permeabilization assay	S14-S15
2.8. Sterol profile by GC-MS	S15-S16
3. References	S16
4. Supplementary Figures (S1-S32)	S17-S32

1. Chemistry:

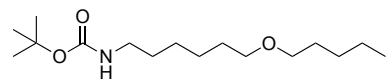
1.1. Materials and instrumentation. All the chemicals used in this study (including compounds **1** and **9**) were purchased from Sigma-Aldrich (St. Louis, MO) or AK Scientific (Union City, CA)

and used without any further purification. DMF and THF were freshly distilled prior to use. Chemical reactions were monitored by TLC (Merck, Silica gel 60 F254). Visualization was achieved using one of the following methods: Iodine stain (I_2 in SiO_2 gel) or UV light. Compounds were purified by SiO_2 flash chromatography (Dynamic Adsorbents Inc., Flash SiO_2 gel 32-63 μ). 1H and ^{13}C NMR spectra were recorded on a Varian 400 MHz spectrometer. Mass spectra were recorded using an Agilent 1200 series Quaternary LC system equipped with a diode array detector, and Eclipse XDB- C_{18} column (250 mm \times 4.6 mm, 5 μ m), and an Agilent 6120 Quadrupole MSD mass spectrometer. For compounds **1** and **2** $[M-Boc+H]^+$ are reported, which correspond to the mass of the molecules that have lost their Boc protecting group during the mass spectrometry experiments. All reactions were carried out under nitrogen atmosphere and all yields reported represent isolated yields. Known compounds were characterized by 1H NMR and are in complete agreement with samples reported in the literature.

1.2. Experimental protocols for the preparation of compounds 1-16.

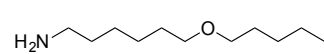


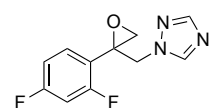
Synthesis of compound 1. To a solution of 6-amino-1-hexanol (700 mg, 5.97 mmol) in CH_2Cl_2 (8 mL), di-*tert*-butyldicarbonate (1.95 g, 8.96 mmol) and Et_3N (1.2 mL, 8.96 mmol) were added. The reaction mixture was stirred at room temperature for 12 h and progress of the reaction was monitored by TLC (1:19/MeOH: CH_2Cl_2 , R_f 0.45). The organic layer was removed under reduced pressure and the residue was purified by column chromatography (SiO_2 , 1:19/MeOH: CH_2Cl_2) to afford compound **1** (1.02 g, 79%) as a colorless liquid: 1H NMR (400 MHz, CD_3OD , Fig. S1) δ 3.52 (t, J = 6.6 Hz, 2H), 3.00 (t, J = 7.0 Hz, 2H), 1.58-1.46 (m, 2H), 1.44-1.42 (m, 2H), 1.41 (s, 9H), 1.38-1.26 (m, 4H); ^{13}C NMR (100 MHz, CD_3OD , Fig. S2) δ 157.1, 78.3, 61.4, 39.9, 32.1, 29.5, 27.4, 26.2, 25.2; LRMS m/z calcd for $C_{11}H_{23}NO_3$: 217.2; found 117.2 $[M-Boc+H]^+$.



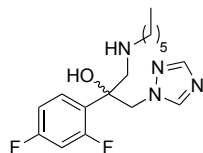
Synthesis of compound 2. A solution of compound **1** (500 mg, 2.30 mmol) in DMF (5 mL) was cooled to 0 $^{\circ}C$ followed by the addition of sodium hydride (72 mg, 2.99 mmol) and 1-iodopentane (0.4 mL, 2.99 mmol). The reaction mixture was stirred at room temperature for 24 h and progress of the reaction was monitored by TLC (1:19/EtOAc:Hexanes, R_f 0.65). The reaction mixture was quenched with H_2O (20 mL) and extracted with EtOAc (60 mL). The organic layer was washed with H_2O (60

mL) and brine (20 mL), and dried over MgSO₄. The organic layer was removed under reduced pressure and the residue was purified by column chromatography (SiO₂, 1:19/EtOAc:Hexanes) to afford compound **2** (241 mg, 36%) as a colorless liquid: ¹H NMR (400 MHz, CD₃OD, Fig. S3) δ 3.39 (td, *J*₁ = 6.6 Hz, *J*₂ = 1.8 Hz, 4H), 3.00 (t, *J* = 7.0 Hz, 2H), 1.56-1.50 (m, 4H), 1.46-1.42 (m, 2H), 1.41 (s, 9H), 1.38-1.26 (m, 8H), 0.90 (m, 3H); ¹³C NMR (100 MHz, CD₃OD, Fig. S4) δ 157.1, 78.3, 70.5, 70.4, 39.9, 29.5, 29.3, 29.0, 28.1, 27.4, 26.3, 25.5, 22.1, 13.0; LRMS *m/z* calcd for C₁₆H₃₃NO₃: 287.3; found 187.2 [M-Boc+H]⁺.

 **Synthesis of compound 3.** To a solution of compound **2** (200 mg, 0.69 mmol) in CH₂Cl₂ (2 mL), trifluoroacetic acid (1.5 mL) was added. The reaction mixture was stirred at room temperature for 2 h and progress of the reaction was monitored by TLC (1:19/MeOH:CH₂Cl₂, *R_f* 0.25). The organic layer was removed under reduced pressure to afford compound **3** (118 mg, 90%) as a colorless liquid: ¹H NMR (400 MHz, CD₃OD, Fig. S5) δ 3.40 (q, *J* = 6.4 Hz, 4H), 2.89 (t, *J* = 7.7 Hz, 2H), 1.65-1.61 (m, 2H), 1.59-1.50 (m, 4H), 1.40 (p, *J* = 3.7 Hz, 4H), 1.31 (p, *J* = 3.7 Hz, 4H), 0.90 (m, 3H); ¹³C NMR (100 MHz, CD₃OD, Fig. S6) δ 70.5, 70.2, 39.2, 29.0 (2C), 28.1, 27.1, 25.8, 25.3, 22.1, 12.9; LRMS *m/z* calcd for C₁₁H₂₅NO: 187.2; found 188.2 [M+H]⁺.

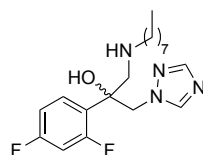
 **Synthesis of compound 4.** To a solution of 2,4-difluoro-2-(1H-1,2,4-triazol-1-yl)acetophenone (1 g, 4.48 mmol) in toluene (10 mL), trimethylsulfoxonium iodide (1.08 g, 4.93 mmol), hexadecyltrimethylammonium bromide (163 mg, 0.45 mmol) and 1.5 mL 20% (v/v) sodium hydroxide was added. The reaction mixture was stirred at 60 °C for 1 h and progress of the reaction was monitored by TLC (3:2/EtOAc:Hexanes, *R_f* 0.35). The reaction mixture was diluted with EtOAc (20 mL) and washed with H₂O (20 mL). The organic layer was removed under reduced pressure and the residue was purified by flash column chromatography (SiO₂, 3:2/EtOAc:Hexanes) to afford compound (720 mg, 68%) as a yellow gummy liquid: ¹H NMR (400 MHz, CDCl₃, Fig. S7) δ 8.08 (s, 1H), 7.86 (s, 1H), 7.20-7.11 (m, 1H), 6.86-6.75 (m, 2H), 4.82 (d, *J* = 14.8 Hz, 1H), 4.49 (d, *J* = 14.8 Hz, 1H), 2.93 (d, *J* = 4.6 Hz, 1H), 2.87 (d, *J* = 4.6 Hz, 1H); ¹³C NMR (100 MHz, CDCl₃, Fig. S8) δ 164.4, 164.3, 161.9, 161.8, 161.7, 159.4, 159.2, 151.8, 144.1, 129.64, 129.59, 129.55, 129.49, 111.90, 111.87, 111.69, 111.65, 104.3,

104.1, 103.8, 56.3, 53.59, 53.55, 52.2; LRMS m/z calcd for $C_{11}H_9F_2N_3O$: 237.1; found 238.1 $[M+H]^+$.



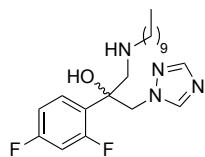
Synthesis of compound 5. To a solution of compound 4 (50 mg, 0.21 mmol) in EtOH (3 mL), hexylamine (0.07 mL, 0.32 mmol) and Et_3N (0.04 mL, 0.32 mmol) were added. The reaction mixture was stirred at 80 °C for 12 h and

progress of the reaction was monitored by TLC (3:2/EtOAc:Hexanes, R_f 0.09). The organic layer was removed under reduced pressure and the residue was purified by column chromatography (SiO_2 , 3:2/EtOAc:Hexanes) to afford compound 5 (11 mg, 14%) as a colorless liquid: 1H NMR (400 MHz, $CDCl_3$, Fig. S9) δ 8.10 (s, 1H), 7.81 (s, 1H), 7.60-7.46 (m, 1H), 6.85-6.75 (m, 2H), 4.65 (d, $J = 14.2$ Hz, 1H), 4.52 (d, $J = 14.2$ Hz, 1H), 3.20 (d, $J = 12.6$ Hz, 1H), 3.00 (d, $J = 12.6$ Hz, 1H), 2.56 (t, $J = 7.2$ Hz, 2H), 1.42-1.38 (p, $J = 7.6$ Hz, 2H), 1.28-1.16 (m, 6H), 0.85 (t, $J = 6.8$ Hz, 3H); ^{13}C NMR (100 MHz, $CDCl_3$, Fig. S10) δ 166.5, 164.1, 153.2, 153.1, 151.8, 151.4, 144.5, 124.93, 124.92, 124.0, 123.9, 110.0, 104.1, 103.8, 95.6, 95.4, 78.1, 63.4, 56.0, 49.8, 47.9, 31.5, 31.4, 29.7, 26.8, 26.7, 26.5, 22.6, 22.5, 14.1, 14.0, 13.9; LRMS m/z calcd for $C_{17}H_{24}F_2N_4O$: 338.2; found 338.3 $[M+H]^+$.

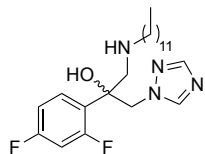


Synthesis of compound 6. To a solution of compound 4 (80 mg, 0.33 mmol) in EtOH (3 mL), *n*-octylamine (0.12 mL, 0.51 mmol) and Et_3N (0.07 mL, 0.51 mmol) were added. The reaction mixture was stirred at 80 °C for 12 h and

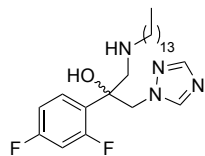
progress of the reaction was monitored by TLC (3:2/EtOAc:Hexanes, R_f 0.20). The organic layer was removed under reduced pressure and the residue was purified by flash column chromatography (SiO_2 , 3:2/EtOAc:Hexanes) to afford compound 6 (85 mg, 70%) as a colorless liquid: 1H NMR (400 MHz, $CDCl_3$, Fig. S11) δ 8.10 (s, 1H), 7.81 (s, 1H), 7.60-7.49 (m, 1H), 6.85-6.75 (m, 2H), 4.63 (d, $J = 14.3$ Hz, 1H), 4.51 (d, $J = 14.3$ Hz, 1H), 3.18 (d, $J = 12.6$ Hz, 1H), 2.95 (d, $J = 12.6$ Hz, 1H), 2.52 (t, $J = 7.2$ Hz, 2H), 1.42-1.36 (m, 2H), 1.29-1.18 (m, 10H), 0.85 (t, $J = 6.6$ Hz, 3H); ^{13}C NMR (100 MHz, $CDCl_3$, Fig. S12) δ 164.0, 163.9, 161.6, 161.4, 160.2, 160.1, 157.8, 157.7, 151.3, 144.7, 129.9, 129.83, 129.79, 129.7, 124.99, 124.86, 111.7, 111.6, 111.44, 111.41, 104.5, 104.22, 104.20, 104.0, 73.0, 72.9, 56.1, 56.0, 54.13, 54.09, 50.0, 31.7, 29.5, 29.3, 29.1, 26.9, 22.6, 14.1; LRMS m/z calcd for $C_{19}H_{28}F_2N_4O$: 366.2; found 367.2 $[M+H]^+$.



Synthesis of compound 7. To a solution of compound **4** (50 mg, 0.21 mmol) in EtOH (3 mL), *n*-decylamine (0.06 mL, 0.32 mmol) and Et₃N (0.04 mL, 0.32 mmol) were added. The reaction mixture was stirred at 80 °C for 12 h and progress of the reaction was monitored by TLC (3:2/EtOAc:Hexanes, R_f 0.20). The organic layer was removed under reduced pressure and the residue was purified by column chromatography (SiO₂, 3:2/EtOAc:Hexanes) to afford compound **7** (75 mg, 91%) as a yellow liquid: ¹H NMR (400 MHz, CD₃OD, Fig. S13) δ 8.32 (s, 1H), 7.76 (s, 1H), 7.48-7.42 (m, 1H), 6.96-6.82 (m, 2H), 4.69 (d, *J* = 14.3 Hz, 1H), 4.61 (d, *J* = 14.3 Hz, 1H), 3.15 (dd, *J*₁ = 12.6 Hz, *J*₂ = 1.4 Hz 1H), 2.98 (dd, *J*₁ = 12.6 Hz, *J*₂ = 1.4 Hz 1H), 2.56-2.44 (m, 2H), 1.42 (p, *J* = 7.2 Hz, 2H), 1.34-1.25 (m, 14H), 0.90 (t, *J* = 6.6 Hz, 3H); ¹³C NMR (100 MHz, CD₃OD, Fig. S14) δ 164.0, 163.9, 161.6, 161.5, 160.6, 160.5, 158.2, 158.1, 149.8, 144.6, 129.8, 129.73, 129.69, 129.6, 125.02, 124.98, 124.8, 110.71, 110.68, 110.50, 110.47, 103.8, 103.6, 103.5, 103.3, 73.83, 73.78, 55.92, 55.87, 54.92, 54.87, 49.8, 31.6, 29.30, 29.26, 29.25, 29.1, 29.0, 26.8, 22.3, 13.0; LRMS *m/z* calcd for C₂₁H₃₂F₂N₄O: 394.3; found 395.2 [M+H]⁺.



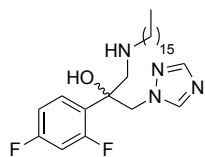
Synthesis of compound 8. To a solution of compound **4** (50 mg, 0.21 mmol) in EtOH (3 mL), dodecylamine (0.07 mL, 0.32 mmol) and Et₃N (0.04 mL, 0.32 mmol) were added. The reaction mixture was stirred at 80 °C for 2 h and progress of the reaction was monitored by TLC (1:10/MeOH:CH₂Cl₂, R_f 0.19). The organic layer was removed under reduced pressure and the residue was purified by column chromatography (SiO₂, 1:10/MeOH:CH₂Cl₂) to afford compound **8** (49 mg, 59%) as a yellow solid: ¹H NMR (400 MHz, CDCl₃, Fig. S15) δ 8.09 (s, 1H), 7.82 (s, 1H), 7.59-7.53 (m, 1H), 6.85-6.76 (m, 2H), 4.67 (d, *J* = 14.2 Hz, 1H), 4.54 (d, *J* = 14.2 Hz, 1H), 3.23 (d, *J* = 12.6 Hz, 1H), 3.08 (d, *J* = 12.6 Hz, 1H), 2.60 (t, *J* = 7.4 Hz, 2H), 1.49-1.43 (m, 2H), 1.29-1.21 (m, 18H), 0.86 (t, *J* = 6.4 Hz, 3H); ¹³C NMR (100 MHz, CDCl₃, Fig. S16) δ 164.0, 161.5, 161.4, 160.2, 160.1, 157.8, 157.7, 151.2, 144.7, 129.9, 129.84, 129.80, 129.7, 125.04, 125.00, 124.9, 111.62, 111.58, 111.41, 111.38, 104.5, 104.20, 104.19, 103.9, 73.0, 72.9, 56.1, 56.0, 54.2, 54.2, 54.1, 50.0, 31.9, 29.7, 29.60, 29.59, 29.54, 29.5, 29.4, 29.34, 29.30, 26.9, 22.7, 14.1; LRMS *m/z* calcd for C₂₃H₃₆F₂N₄O: 422.3; found 423.2 [M+H]⁺.



Synthesis of compound 9. To a solution of compound **4** (50 mg, 0.21 mmol)

in EtOH (3 mL), tetradecylamine (68 mg, 0.32 mmol) and Et₃N (0.04 mL, 0.32 mmol) were added. The reaction mixture was stirred at room temperature for 3

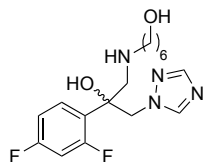
h and progress of the reaction was monitored by TLC (1:10/MeOH:CH₂Cl₂, R_f 0.31). The organic layer was removed under reduced pressure and the residue was purified by column chromatography (SiO₂, 1:10/MeOH:CH₂Cl₂) to afford compound **9** (90 mg, 94%) as a yellow liquid: ¹H NMR (400 MHz, CD₃OD, Fig. S17) δ 8.29 (s, 1H), 7.74 (s, 1H), 7.46-7.40 (m, 1H), 6.93-6.80 (m, 2H), 4.67 (d, *J* = 14.3 Hz, 1H), 4.59 (d, *J* = 14.3 Hz, 1H), 3.13 (dd, *J*₁ = 12.6 Hz, *J*₂ = 1.3 Hz, 1H), 2.96 (dd, *J*₁ = 12.6 Hz, *J*₂ = 1.3 Hz, 1H), 2.54-2.42 (m, 2H), 1.42-1.36 (p, *J* = 7.1 Hz, 2H), 1.32-1.23 (m, 22H), 0.88 (t, *J* = 6.6 Hz, 3H); ¹³C NMR (100 MHz, CD₃OD, Fig. S18) δ 164.0, 163.9, 161.6, 160.6, 160.5, 158.2, 158.1, 149.7, 144.6, 129.8, 129.72, 129.69, 129.6, 125.0, 124.8, 110.71, 110.68, 110.50, 110.47, 103.8, 103.6, 103.5, 103.3, 73.82, 73.76, 55.9, 55.85, 54.91, 54.86, 49.8, 31.7, 29.37, 29.35, 29.34, 29.28, 29.27, 29.14, 29.10, 29.06, 26.8, 22.3, 13.0; LRMS *m/z* calcd for C₂₅H₄₀F₂N₄O: 450.3; found 451.3 [M+H]⁺.



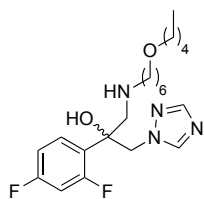
Synthesis of compound 10. To a solution of compound **4** (50 mg, 0.21 mmol)

in EtOH (3 mL), hexadecylamine (76 mg, 0.32 mmol) and Et₃N (0.04 mL, 0.32 mmol) were added. The reaction mixture was stirred at room temperature

for 2 h and progress of the reaction was monitored by TLC (1:10/MeOH:CH₂Cl₂, R_f 0.29). The organic layer was removed under reduced pressure and the residue was purified by column chromatography (SiO₂, 1:10/MeOH:CH₂Cl₂) to afford compound **10** (92 mg, 91%) as a yellow liquid: ¹H NMR (400 MHz, CD₃OD, Fig. S19) δ 8.29 (s, 1H), 7.74 (s, 1H), 7.47-7.40 (m, 1H), 6.93-6.80 (m, 2H), 4.67 (d, *J* = 14.3 Hz, 1H), 4.59 (d, *J* = 14.3 Hz, 1H), 3.13 (dd, *J*₁ = 12.6 Hz, *J*₂ = 1.3 Hz, 1H), 2.96 (dd, *J*₁ = 12.6 Hz, *J*₂ = 1.3 Hz, 1H), 2.54-2.41 (m, 2H), 1.40 (p, *J* = 7.1 Hz, 2H), 1.32-1.23 (m, 26H), 0.88 (t, *J* = 6.7 Hz, 3H); ¹³C NMR (100 MHz, CD₃OD, Fig. S20) δ 164.0, 163.9, 161.6, 161.4, 160.6, 160.5, 158.2, 158.1, 150.6, 149.7, 144.6, 129.8, 129.72, 129.69, 129.63, 125.02, 124.98, 124.89, 124.85, 110.71, 110.68, 110.50, 110.47, 103.8, 103.6, 103.5, 103.3, 73.83, 73.78, 55.91, 55.86, 54.94, 54.90, 49.8, 31.7, 29.39, 29.37, 29.35, 29.30, 29.28, 29.2, 29.1, 26.8, 22.3, 13.0; LRMS *m/z* calcd for C₂₇H₄₄F₂N₄O: 478.4; found 479.3 [M+H]⁺.

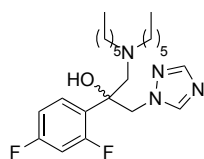


Synthesis of compound 11. To a solution of compound **4** (50 mg, 0.21 mmol) in EtOH (3 mL), 6-amino-1-hexanol (37 mg, 0.32 mmol) and Et₃N (0.04 mL, 0.32 mmol) were added. The reaction mixture was stirred at room temperature for 12 h and progress of the reaction was monitored by TLC (1:20/MeOH:CH₂Cl₂, R_f 0.66). The organic layer was removed under reduced pressure and the residue was purified by column chromatography (SiO₂, 1:20/MeOH:CH₂Cl₂) to afford compound **11** (35 mg, 51%) as a colorless liquid: ¹H NMR (400 MHz, CD₃OD, Fig. S21) δ 8.31 (s, 1H), 7.80 (s, 1H), 7.52-7.45 (m, 1H), 7.00-6.95 (m, 1H), 6.93-6.87 (m, 1H), 4.71 (d, *J* = 14.5 Hz, 1H), 4.66 (d, *J* = 14.5 Hz, 1H), 3.51 (t, *J* = 6.5 Hz, 2H), 3.40 (d, *J* = 12.8 Hz, 1H), 3.20 (d, *J* = 12.8 Hz, 1H), 2.77-2.65 (m, 2H), 1.56-1.45 (m, 4H), 1.38-1.25 (m, 4H); ¹³C NMR (100 MHz, CD₃OD, Fig. S22) δ 164.5, 164.4, 162.0, 161.9, 160.7, 160.6, 158.3, 158.2, 150.2, 144.8, 129.92, 129.86, 129.82, 129.76, 123.2, 111.14, 111.11, 110.93, 110.90, 104.2, 103.9, 103.6, 73.1, 73.0, 61.3, 55.52, 55.47, 53.8, 53.7, 49.1, 32.0, 27.1, 26.3, 25.2; LRMS *m/z* calcd for C₁₇H₂₄F₂N₄O₂: 354.2; found 355.1 [M+H]⁺.



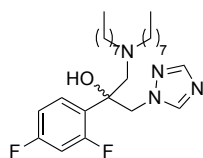
Synthesis of compound 12. To a solution of compound **4** (50 mg, 0.21 mmol) in EtOH (3 mL), compound **3** (60 mg, 0.32 mmol) and Et₃N (0.04 mL, 0.32 mmol) were added. The reaction mixture was stirred at 80 °C for 12 h and progress of the reaction was monitored by TLC (3:2/EtOAc:Hexanes, R_f 0.30).

The organic layer was removed under reduced pressure and the residue was purified by column chromatography (SiO₂, 3:2/EtOAc:Hexanes) to afford compound **12** (34 mg, 39%) as a yellow liquid: ¹H NMR (400 MHz, CD₃OD, Fig. S23) δ 8.29 (s, 1H), 7.75 (s, 1H), 7.47-7.40 (m, 1H), 6.95-6.80 (m, 2H), 4.67 (d, *J* = 14.3 Hz, 1H), 4.60 (d, *J* = 14.3 Hz, 1H), 3.39 (t, *J* = 6.6 Hz, 2H), 3.38 (t, *J* = 6.6 Hz, 2H), 3.16 (d, *J* = 12.6 Hz, 1H), 2.99 (d, *J* = 12.6 Hz, 1H), 2.59-2.43 (m, 2H), 1.58-1.46 (m, 4H), 1.43 (p, *J* = 6.9 Hz, 2H), 1.36-1.22 (m, 8H), 0.89 (t, *J* = 6.2 Hz, 3H); ¹³C NMR (100 MHz, CD₃OD, Fig. S24) δ 164.1, 161.6, 158.2, 149.8, 144.6, 129.8, 129.7, 129.6, 124.8, 110.7, 110.6, 103.9, 103.6, 103.3, 73.73, 73.67, 70.5, 70.3, 55.9, 55.8, 54.8, 54.7, 49.7, 29.2, 29.0, 28.8, 28.1, 26.6, 25.6, 22.1, 13.0; LRMS *m/z* calcd for C₂₂H₃₄F₂N₄O₂: 424.3; found 425.2 [M+H]⁺.



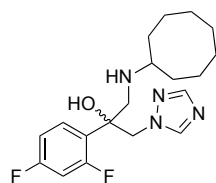
Synthesis of compound 13. To a solution of compound **4** (80 mg, 0.33 mmol) in EtOH (3 mL), di-*n*-hexylamine (0.12 mL, 0.51 mmol) and Et₃N (0.07 mL,

0.51 mmol) were added. The reaction mixture was stirred at 80 °C for 12 h and progress of the reaction was monitored by TLC (3:2/EtOAc:Hexanes, R_f 0.82). The organic layer was removed under reduced pressure and the residue was purified by flash column chromatography (SiO₂, 1:4/EtOAc:Hexanes) to afford compound **13** (82 mg, 57%) as a colorless liquid: ¹H NMR (400 MHz, CDCl₃, Fig. S25) δ 8.17 (s, 1H), 7.77 (s, 1H), 7.55 (m, 1H), 6.85-6.74 (m, 2H), 5.66 (br s, 1H), 4.50 (d, J = 14.1 Hz, 1H), 4.41 (d, J = 14.1 Hz, 1H), 3.05 (d, J = 13.7 Hz, 1H), 2.69 (d, J = 13.7 Hz, 1H), 2.26-2.04 (m, 4H), 1.25-0.98 (m, 16H), 0.83 (t, J = 7.2 Hz, 6H); ¹³C NMR (100 MHz, CDCl₃, Fig. S26) δ 160.2, 160.1, 157.7, 157.6, 150.8, 144.8, 129.5, 127.1, 111.4, 111.2, 104.4, 104.1, 103.9, 71.0, 58.9, 56.52, 56.47, 55.0, 31.5, 26.8, 26.7, 22.5, 13.9; LRMS m/z calcd for C₂₃H₃₆F₂N₄O: 422.3; found 423.2 [M+H]⁺.



Synthesis of compound 14. To a solution of compound **4** (50 mg, 0.21 mmol) in EtOH (3 mL), di-*n*-octylamine (0.09 mL, 0.32 mmol) and Et₃N (0.04 mL, 0.32 mmol) were added. The reaction mixture was stirred at 80 °C for 12 h and

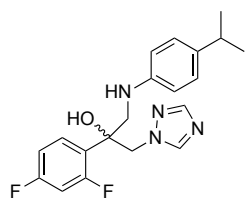
progress of the reaction was monitored by TLC (3:2/EtOAc:Hexanes, R_f 0.60). The organic layer was removed under reduced pressure and the residue was purified by flash column chromatography (SiO₂, 1:4/EtOAc:Hexanes) to afford compound **14** (65 mg, 65%) as a yellow liquid: ¹H NMR (400 MHz, CD₃OD, Fig. S27) δ 8.39 (s, 1H), 7.79 (s, 1H), 7.60-7.54 (m, 1H), 6.98-6.85 (m, 2H), 4.59 (d, J = 14.3 Hz, 1H), 4.55 (d, J = 14.3 Hz, 1H), 3.09 (dd, J_1 = 13.9 Hz, J_2 = 1.8 Hz, 1H), 2.81 (d, J = 13.9 Hz, 1H), 2.34-2.20 (m, 4H), 1.34-1.05 (m, 24H), 0.90 (t, J = 6.7 Hz, 6H); ¹³C NMR (100 MHz, CD₃OD, Fig. S28) δ 164.1, 163.9, 161.6, 161.5, 160.5, 160.4, 158.0, 157.9, 149.6, 144.9, 129.61, 129.55, 129.52, 129.46, 126.95, 126.91, 126.82, 126.78, 110.8, 110.7, 110.6, 110.5, 103.8, 103.57, 103.56, 103.3, 71.7, 71.6, 59.23, 59.19, 56.1, 56.0, 54.9, 31.5, 29.0, 28.9, 26.8, 26.6, 22.3, 13.0; LRMS m/z calcd for C₂₇H₄₄F₂N₄O: 478.4; found 479.3 [M+H]⁺.



Synthesis of compound 15. To a solution of compound **4** (50 mg, 0.21 mmol) in EtOH (3 mL), cyclooctylamine (0.04 mL, 0.32 mmol) and Et₃N (0.04 mL, 0.32 mmol) were added. The reaction mixture was stirred at 80 °C for 2 h and

progress of the reaction was monitored by TLC (1:20/MeOH:CH₂Cl₂, R_f 0.52). The organic layer was removed under reduced pressure and the residue was purified by

column chromatography (SiO₂, 1:20/MeOH:CH₂Cl₂) to afford compound **15** (43 mg, 57%) as a colorless liquid: ¹H NMR (400 MHz, CDCl₃, Fig. S29) δ 8.11 (s, 1H), 7.81 (s, 1H), 7.59-7.53 (m, 1H), 6.85-6.75 (m, 2H), 4.62 (d, *J* = 14.2 Hz, 1H), 4.48 (d, *J* = 14.2 Hz, 1H), 3.14 (d, *J* = 12.6 Hz, 1H), 2.96 (d, *J* = 12.6 Hz, 1H), 2.53 (br s, 1H), 2.02-1.22 (m, 15H); ¹³C NMR (100 MHz, CDCl₃, Fig. S30) δ 164.0, 163.9, 161.5, 161.4, 160.3, 160.2, 157.8, 157.7, 151.2, 144.8, 129.9, 129.82, 129.78, 129.7, 125.3, 125.2, 111.6, 111.5, 111.4, 111.3, 104.4, 104.2, 103.9, 72.63, 72.58, 58.0, 56.24, 56.19, 51.73, 51.69, 32.6, 32.1, 27.1, 27.0, 25.6, 23.8, 23.6; LRMS *m/z* calcd for C₁₉H₂₆F₂N₄O: 364.2; found 365.1 [M+H]⁺.



Synthesis of compound 16. To a solution of compound **4** (50 mg, 0.21 mmol) in EtOH (3 mL), 4-isopropylaniline (0.04mL, 0.32 mmol) and Et₃N (0.04 mL, 0.32 mmol) were added. The reaction mixture was stirred at 80 °C for 2 h and progress of the reaction was monitored by TLC

(1:10/MeOH:CH₂Cl₂, *R_f* 0.88). The organic layer was removed under reduced pressure and the residue was purified by column chromatography (SiO₂, 1:20/MeOH:CH₂Cl₂) to afford compound **16** (45 mg, 57%) as a yellow solid: ¹H NMR (400 MHz, CDCl₃, Fig. S31) δ 7.96 (s, 1H), 7.83 (s, 1H), 7.53-7.47 (m, 1H), 7.03 (d, *J* = 8.4 Hz, 1H), 6.81-6.73 (m, 2H), 6.63 (d, *J* = 8.4 Hz, 2H), 4.76 (d, *J* = 14.2 Hz, 1H), 4.70 (d, *J* = 14.2 Hz, 1H), 3.64 (dd, *J*₁ = 13.1 Hz, *J*₂ = 1.3 Hz, 1H), 3.51 (dd, *J*₁ = 13.1 Hz, *J*₂ = 1.3 Hz, 1H), 2.79 (septet, *J* = 6.9 Hz, 1H), 1.17 (d, *J* = 6.9 Hz, 6H); ¹³C NMR (100 MHz, CDCl₃, Fig. S32) δ 164.1, 164.0, 161.6, 161.5, 159.9, 159.8, 157.5, 157.4, 151.9, 145.4, 144.4, 139.6, 130.1, 130.04, 130.00, 129.9, 127.2, 124.04, 124.00, 123.91, 123.87, 114.0, 111.91, 111.88, 111.71, 111.68, 104.5, 104.27, 104.26, 104.0, 75.7, 75.6, 55.2, 55.1, 51.24, 51.20, 33.2, 24.2; LRMS *m/z* calcd for C₂₀H₂₂F₂N₄O: 372.2; found 373.1 [M+H]⁺.

2. Biological studies:

2.1. Antifungal agents. Azole derivatives **5-16** were chemically synthesized as described in section 1.2 above. A 5 mg/mL stock solution of compounds **5-16** was prepared in DMSO and stored at -20 °C. The antifungal agents amphotericin B (AmB), fluconazole (FLC), and voriconazole (VOR) were obtained from AK Scientific Inc. (Mountain View, CA). The antifungal agent caspofungin (CAS) was purchased from Sigma-Aldrich (St. Louis, MO). AmB,

FLC, VOR, and CAS were dissolved in DMSO at a final concentration of 5 mg/mL and were stored at -20 °C.

2.2. Organisms and culture conditions. *Candida albicans* ATCC 10231 (**A**), *C. albicans* ATCC 64124 (**B**), and *C. albicans* ATCC MYA-2876 (**C**) were kindly provided by Dr. Jon Y. Takemoto (Utah State University, Logan, UT, USA). *C. albicans* ATCC MYA-90819 (**D**), *C. albicans* ATCC MYA-2310 (**E**), *C. albicans* ATCC MYA-1237 (**F**), *C. albicans* ATCC MYA-1003 (**G**), *Candida glabrata* ATCC 2001 (**H**), *Candida krusei* ATCC 6258 (**I**), *Candida parapsilosis* ATCC 22019 (**J**), *Aspergillus flavus* ATCC MYA-3631 (**K**), and *Aspergillus terreus* ATCC MYA-3633 (**M**) were obtained from the American Type Culture Collection (ATCC; Manassas, VA, USA). *Aspergillus nidulans* ATCC 38163 (**L**) was received from Dr. Jon S. Thorson (University of Kentucky, Lexington, KY, USA). All clinical fungal isolates, *C. glabrata* (**CG1**, **CG2**, and **CG3**), *C. parapsilosis* (**CP1**, **CP2**, **CP3**), and *Cryptococcus neoformans* (**CN1**, **CN2**, and **CN3**) were obtained from Dr. Nathan P. Wiederhold, University of Texas Health Science Center, San Antonio, USA). Filamentous fungi and yeasts were cultivated at 35 °C in RPMI 1640 medium (with L-glutamine, without sodium bicarbonate, Sigma-Aldrich, St. Louis, MO, USA) buffered to a pH of 7.0 with 0.165 M morpholinepropanesulfonic acid (MOPS) buffer (Sigma-Aldrich).

The human embryonic kidney cell line HEK-293 (ATCC CRL-1573), the human bronchus normal cell line BEAS-2B (ATCC CRL-9609), and the human lung carcinoma cell line A549 (ATCC CRL-185) were kind gifts from the laboratories of Dr. Matthew S. Gentry (University of Kentucky, Lexington, KY, USA) and Dr. David K. Orren (University of Kentucky, Lexington, KY, USA). Mammalian cells were grown in Dulbecco's Modified Eagle's Medium (DMEM) (from ATCC) with 10% fetal bovine serum (FBS) (from ATCC) and 1% Pen/Strep (from ATCC). Cell lines were incubated at 37 °C and 5% CO₂ and passaged by trypsinization with 0.05% trypsin:0.53 mM EDTA (from ATCC). Cell confluency was determined by using a Nikon Eclipse TS100 microscope (Minato, Tokyo, Japan).

2.3. Antifungal susceptibility testing. The MIC values of compounds **5-16** against yeasts (strains **A-J** (Table 1), and **CG1-3**, **CP1-3**, and **CN1-3** (Table 2)) were evaluated in 96-well

microtiter plates as described in the CLSI document M27-A3¹ with minor modifications. The final concentrations of antifungal agents studied ranged from 0.03-31.3 µg/mL for compounds **5-16**, 0.48-31.3 µg/mL for AmB (only presented in Table 1), 0.03-31.3 µg/mL for CAS, 0.975-62.5 µg/mL for FLC, and 0.03-31.3 µg/mL for VOR. Briefly, overnight yeast cultures were grown in yeast peptone dextrose (YPD) broth and the cell density was adjusted to an OD₆₀₀ of 0.12 (~1×10⁶ CFU/mL) by using a spectrophotometer. Yeast cell suspensions were further diluted to achieve 1-5×10³ CFU/mL in RPMI 1640 medium, and 100 µL of these yeast cells was added to 96-well microtiter plates containing RPMI 1640 medium and titrated compounds. Each test was performed in triplicate. The plates were incubated at 35 °C for 48 h. The MIC values for compounds **5-16**, AmB, and CAS were defined as the lowest drug concentration that prevented visible growth (also known as MIC-0) when compared to the growth control. For FLC and VOR, the minimum drug concentration that yielded at least 50% growth inhibition (MIC-2) when compared with the growth control well was reported. One exception for the reporting of the MIC of the azoles was that of VOR against *C. albicans* ATCC 10231 (strain **A**), where the MIC-0 (indicating optically clear well) was reported. These data are presented in Tables 1 (MIC values in µg/mL) and S1 (MIC values in µM) (for strains **A-J**) and 2 (MIC values in µg/mL) and S2 (MIC values in µM) (for strains **CG1-3**, **CP1-3**, and **CN1-3**).

Similarly, the MIC values of compounds **5-16**, as well as that of all control drugs against filamentous fungi (strains **K-M**) were determined as previously described in CLSI document M38-A2.² Spores were harvested from sporulating cultures growing on potato dextrose agar (PDA) by filtration through sterile glass wool and enumerated by using a hemocytometer (Hausser Scientific, PA, USA) to obtain the desired inoculum size. Two-fold serial dilutions of compounds **5-16**, as well as VOR and CAS were made in sterile 96-well microtiter plates in the range of 0.03-31.3 µg/mL in RPMI 1640 medium. The concentration range for FLC and AmB were 0.975-62.5 µg/mL and 0.48-31.3 µg/mL, respectively. Spore suspensions were added to the wells to afford a final concentration of 5×10⁵ spores/mL. The plates were incubated at 35 °C for 48 h. The MIC values of all compounds, including compounds **5-16**, azoles, AmB, and CAS against filamentous fungi were based on complete inhibition of growth (optically clear well) when compared to the growth control (MIC-0). Each test was performed in triplicate. These data are also presented in Table 1 (strains **K-M**).

Table S1: MIC values^a (in μM) (the corresponding values in $\mu\text{g/mL}$ are presented in Table 1) determined for compounds **5-16** and for four control antifungal agents (AmB, CAS, FLC, and VOR) against various yeast strains and filamentous fungi.

Cpd #	Yeast strains										Filamentous fungi		
	A	B	C	D	E	F	G	H	I	J	K	L	M
5	23.0	>92.3	46.1	92.3	92.3	>92.3	92.3	46.1	23.0	2.9	>92.3	>92.3	>92.3
6	2.7	>85.4	85.4	21.3	85.4	42.6	85.4	21.3	2.7	0.16	>85.4	5.3	42.6
7	1.2	39.5	9.9	9.9	19.8	19.8	19.8	2.5	1.2	0.08	19.8	2.5	9.9
8	2.3	76.0	9.2	4.6	76.0	18.5	76.0	2.3	2.3	1.1	18.5	4.6	9.2
9	4.3	>69.5	>69.5	17.3	69.5	>69.5	69.5	2.2	8.7	1.1	>69.5	8.7	17.3
10	>65.4	>65.4	65.4	65.4	8.1-65.4	>65.4	>65.4	2.0	8.1	1.0	>65.4	8.1	>65.4
11	>88.3	>88.3	88.3	88.3	>88.3	>88.3	>88.3	>88.3	>88.3	>88.3	>88.3	>88.3	>88.3
12	9.2	>73.7	73.7	9.2	36.7	9.2	18.4	36.7	4.6	0.57	>73.7	18.4	73.7
13	>74.1	>74.1	>74.1	>74.1	>74.1	>74.1	>74.1	>74.1	>74.1	74.1	>74.1	>74.1	>74.1
14	65.4	>65.4	65.4	65.4	>65.4	65.4	>65.4	65.4	65.4	2.0	>65.4	32.7	>65.4
15	85.8	85.8	>85.8	85.8	10.7-85.8	85.8	>85.8	85.8	85.8	10.7	85.8	>85.8	>85.8
16	>84.0	>84.0	>84.0	84.0	84.0	84.0	84.0	20.9	>84.0	20.9	84.0	20.9	41.9
AmB	4.2	4.2	2.1	1.1	2.1	4.2	4.2	2.1	4.2	2.1	15.6	4.2	4.2
CAS	0.8	0.2	0.05	0.1	0.1	0.2	0.4	0.05	0.4	1.6	>25.8	>25.8	>25.8
FLC	204.1	>408.1	50.9	>408.1	>408.1	204.1	204.1	>102.2	>102.2	6.4	204.1	204.1	204.1
VOR	0.69	11.2	5.6	5.6	2.8	22.3	5.6	0.17	0.34	<0.06	0.69	0.34	0.34

Yeast strains: **A** = *Candida albicans* ATCC 10231, **B** = *C. albicans* ATCC 64124, **C** = *C. albicans* ATCC MYA-2876(S), **D** = *C. albicans* ATCC 90819(R), **E** = *C. albicans* ATCC MYA-2310(S), **F** = *C. albicans* ATCC MYA-1237(R), **G** = *C. albicans* ATCC MYA-1003(R), **H** = *Candida glabrata* ATCC 2001, **I** = *Candida krusei* ATCC 6258, **J** = *Candida parapsilosis* ATCC 22019. NOTE: Here, the (S) and (R) indicate that ATCC reports these strains to be susceptible (S) and resistant (R) to ITC and FLC.

Filamentous fungi: **K** = *Aspergillus flavus* ATCC MYA-3631, **L** = *Aspergillus nidulans* ATCC 38163, **M** = *Aspergillus terreus* ATCC MYA-3633.

Known antifungal agents: **AmB** = amphotericin B, **CAS** = caspofungin, **FLC** = fluconazole, **VOR** = voriconazole.

^a For yeast strains: MIC-0 values are reported for FLC analogues **5-16**, AmB, and CAS, whereas MIC-2 values are reported for azoles. For filamentous fungi, MIC-0 values are reported for all compounds.

Table S2: MIC values^a (in μM) (the corresponding values in $\mu\text{g/mL}$ are presented in Table 2) determined for compounds **5-16** and for two control antifungal agents (FLC and VOR) against various non-*albicans* *Candida* and *Cryptococcus neoformans* clinical isolates.

Cpd #	Yeast strains										
	H	CG1	CG2	CG3	J	CP1	CP2	CP3	CN1	CN2	CN3
5	23.0	92.3	23.0	92.3	2.9	2.9	2.9	2.9	23.0	>92.3	92.3
6	2.7	21.3	2.7	42.6	0.16	1.3	0.33	0.65	5.3	10.6	10.6
7	1.2	4.9	1.2	9.9	0.08	0.15	0.30	0.61	0.61	0.61	1.2
8	2.3	4.6	2.3	4.6	1.1	0.14	0.57	0.28	0.57	0.57	1.1
9	4.3	4.3	4.3	8.7	1.1	1.1	2.2	1.1	0.27	0.53	1.1
10	>65.4	4.1	2.0	16.3	1.0	2.0	1.0	2.0	1.0	1.0	1.0
11	>88.3	>88.3	>88.3	>88.3	>88.3	88.3	88.3	88.3	>88.3	>88.3	>88.3
12	9.2	36.7	4.6	73.7	0.57	0.28	0.28	0.28	1.1	4.6	4.6
13	>74.1	>74.1	>74.1	>74.1	74.1	>74.1	>74.1	>74.1	>74.1	>74.1	37.1
14	65.4	32.6	16.3	>65.4	2.0	2.0	4.1	4.1	>65.4	>65.4	>65.4
15	85.8	85.8	42.8	85.8	10.7	2.7	2.7	5.4	21.4	>85.8	42.8
16	>84.0	20.9	20.9	20.9	20.9	10.5	10.5	10.5	20.9	84.0	>84.0
CAS	0.05	0.16	0.2	0.8	1.6	0.4	0.4	0.4	12.9	25.8	12.9
FLC	204.1	>102.1	>102.1	>102.1	6.4	3.2	3.2	3.2	25.6	>102.1	>102.1
VOR	0.69	2.76	11.2	>89.9	<0.06	<0.06	<0.06	<0.06	0.69	2.76	0.35

Yeast strains: **H** = *Candida glabrata* ATCC 2001, **CG1-CG3** = *C. glabrata* clinical isolates, **J** = *Candida parapsilosis* ATCC 22019, **CP1-CP3** = *C. parapsilosis* clinical isolates, **CN1-CN3** = *Cryptococcus neoformans* clinical isolates.

Known antifungal agents: **CAS** = caspofungin, **FLC** = fluconazole, **VOR** = voriconazole.

^a For these yeast strains: MIC-0 values are reported for FLC analogues **5-16**, whereas MIC-2 values are reported for azoles.

2.4. Time-kill studies. The time-kill curve analyses were done using a previously published protocol.³ Fungal cells (*C. albicans* ATCC 10231 (strain **A**) and *C. parapsilosis* ATCC 22019 (strain **J**)) were cultured in YPD medium (3 mL) overnight. Cells (~10-15 μL) were then added

to Eppendorf tubes and diluted (to 1 mL) with RPMI 1640 medium to achieve the proper concentration of working stocks with OD₆₀₀ of 0.12-0.13. Prior to performing the time-kill studies, cells (300 µL) were aliquoted into 15 mL conical tubes along with 3.7 mL of RPMI 1640 medium (total of 4 mL) to establish that 300 µL from working stock of OD₆₀₀ of 0.12-0.13 would be sufficient to achieve the initial inoculum (time 0 h) of 1-4×10⁵ CFU/mL on PDA plates after at least 24 h incubation. Once established, 300 µL of cells and appropriate volumes of RPMI 1640 medium and compounds (**6**, **7**, and VOR) were then added to make up solutions of cells and drugs with concentrations of 1×, 4×, and 8× the respective MIC values of each compound. The final volume for each tube was 4 mL. The tubes were then incubated at 35 °C and agitated at 200 rpm for 24 h. At 0, 3, 6, 9, 12, and 24 h time points, 100 µL of cells from each tube was serially diluted with RPMI 1640 medium to the appropriate dilutions (10²-10⁷ times) depending on turbidity. Afterwards, the cells were plated on PDA plates. Please note that proper dilution comes with experience and the dilutions were done to make sure that each plate contains 30-300 colonies, which is considered statistically significant. The plates were then incubated for 24-48 h and the number of colonies were counted. The experiments were performed in duplicate. These data are presented in Fig. 3.

2.5. Hemolytic activity assay. The hemolytic activity of compounds **6-10** was determined by using previously described methods with minor modifications.⁴ Murine whole blood was suspended in 4 mL of PBS and centrifuged at 1,000 rpm for 10 min at room temperature to obtain the mRBCs. The mRBCs were washed four times in PBS and resuspended in the same buffer to a final concentration of 10⁷ erythrocytes/mL. Two-fold serial dilutions of compounds **6-10** were prepared using 100 µL of PBS buffer in Eppendorf tubes followed by the addition of 100 µL of mRBC suspension that made the final concentration of compounds and mRBCs to be 0.48-62.5 µg/mL and 5×10⁶ erythrocytes/mL, respectively. The tubes were incubated at 37 °C for 1 h. Tubes with PBS buffer (200 µL) and Triton™ X-100 (1% v/v, 2 µL) served as negative (blank) and positive controls, respectively. The percentage of hemolysis was calculated using the following equation: % hemolysis = [(absorbance of sample) – (absorbance of blank)] × 100/(absorbance of positive control). These data are presented in Table S3 and Fig. 4.

Table S3: The % hemolysis caused by azole derivatives and VOR against mRBCs with the error bars (\pm SDEV).

Cpd #	Concentration ($\mu\text{g/mL}$)							
	0.48	0.975	1.95	3.9	7.8	15.6	31.3	62.5
6	2.0 \pm 0.3	2.0 \pm 1.0	0	2.0 \pm 0.8	0	3.0 \pm 0.3	9.0 \pm 0.3	78.0 \pm 1.0
7	0	0	2.0 \pm 0.1	3.0 \pm 3.0	8.0 \pm 2.0	33.0 \pm 7.0	92.0 \pm 7.0	100.0 \pm 3.0
8	2.0 \pm 0.9	2.0 \pm 0.8	2.0 \pm 1.4	8.0 \pm 4.0	21.0 \pm 5.0	86.0 \pm 11.0	100.0 \pm 5.0	98.0 \pm 2.0
9	2.0 \pm 0.9	6.0 \pm 3.0	3.0 \pm 2.0	10.0 \pm 2.0	17.0 \pm 2.0	29.0 \pm 0.3	57.0 \pm 6.0	77.0 \pm 8.0
10	4.0 \pm 0.2	5.0 \pm 4.2	6.0 \pm 4.0	3.0 \pm 2.0	4.0 \pm 0.2	4.0 \pm 1.0	4.0 \pm 0.5	8.0 \pm 3.0
VOR	9.0 \pm 5.0	10.0 \pm 2.0	6.0 \pm 2.0	7.0 \pm 0.5	11.0 \pm 11.0	3.0 \pm 1.2	83.0 \pm 5.0	100.0 \pm 2.3

2.6. *In vitro* cytotoxicity assay. Mammalian cytotoxicity assays were performed as previously described with minor modifications.⁵ HEK-293, BEAS-2B, and A549 were cultured as described in section 2.2 and were counted by a hemocytometer when cells were about 80% confluent in flasks. Cells were plated in 96-well microtiter plates at concentrations of 10,000 cells per well for HEK-293 and 3,000 cells per well for BEAS-2B and A549. The 96-well microtiter plates were incubated at 37 °C and 5% CO₂ for 16 h to allow time for adherence. The medium was then removed and fresh medium with compounds **6-10** or VOR at 0.13-31 $\mu\text{g/mL}$ and 0.1% DMSO vehicle were added. The stock solutions of compounds **6-10** were previously prepared at 1000 \times the intended tested concentrations. The positive control contained 20% Triton™ X-100. The negative control contained 0.1% DMSO and no drugs. A blank control was also prepared to have only medium and no cells. After 24 h of incubation, cell survival was assessed *via* addition of resazurin (10 μL of 10 mM solution) for 6-10 h. Live cells were detected by a color change from purple to pink *via* conversion of the compound to resorufin, which could be quantified at λ_{560} absorption and λ_{590} emission by a SpectraMax M5 plate reader. The percentage survival rates were calculated by using the following formula: % cell survival = [(fluorescence of sample) – (fluorescence of blank)] \times 100/[(fluorescence of negative control)-(fluorescence of blank)]. The experiments were performed in duplicate. These data are presented in Fig. 5.

2.7. Membrane permeabilization assay. 2 mL of YPD broth was first inoculated using a fresh colony of *C. albicans* ATCC 10231 (strain A) in a sterile culture tube and was grown overnight at 35 °C at 200 rpm. 50 μL of an overnight culture was transferred to RPMI 1640 medium (0.5 mL) containing no drug (negative control) or compound **8** at 1 \times MIC (1.95 $\mu\text{g/mL}$), 2 \times MIC (3.9 $\mu\text{g/mL}$), and 4 \times MIC (7.8 $\mu\text{g/mL}$) or compound **9** at 1 \times MIC (3.9 $\mu\text{g/mL}$), 2 \times MIC (7.8 $\mu\text{g/mL}$), and 4 \times MIC (15.6 $\mu\text{g/mL}$). VOR at 4 \times MIC (0.975 $\mu\text{g/mL}$), and KANB (C₁₄)⁴ at 4 \times MIC (15.6 $\mu\text{g/mL}$) were also used as negative and positive controls, respectively. After establishing that

using 4× MIC was required to display membrane permeabilization, compounds **5**, **6**, and **7** were also tested at their respective 4× MIC (31.2, 3.9, and 1.95 µg/mL, respectively). The cell suspensions were then treated for 1 h at 35 °C with continuous agitation (200 rpm). The cells were then centrifuged and resuspended in 500 µL of PBS buffer (pH 7.2). Subsequently, cells were treated with propidium iodide (9 µM, final concentration) and incubated for 20 min at room temperature in the dark. Glass slides prepared with 10 µL of each mixture were observed in bright field and fluorescence modes (using Texas red filter set, excitation and emission wavelengths of 535 and 617 nm, respectively) using a Zeiss Axiovert 200M fluorescence microscope. A magnification lens of 63X was used. Data were obtained from at least two independent experiments. The images were also post-processed utilizing automatic contrast and brightness setting in Microsoft PowerPoint 2013 to eliminate background noise. These images are presented in Fig. 6.

2.8. Sterol profile by GC-MS. A single colony of *C. albicans* ATCC 10231 (strain **A**) was picked from a fresh culture plate to inoculate 3 mL of yeast peptone dextrose broth (YPDB) and was incubated at 35 °C for ~18 h with continuous agitation (180 rpm). The overnight yeast culture was used to inoculate RPMI 1640 medium (15 mL) and the final inoculum concentration was adjusted to 1×10^6 CFU/mL ($\sim OD_{600} = 0.12$) by using spectrophotometric method. Afterwards, the yeast cells were treated with compounds **8** (0.48 µg/mL), compound **9** (0.975 µg/mL), or VOR (0.12 µg/mL) at their sub-MIC values. An equivalent amount of DMSO without drug (untreated control) was also prepared. Cells were harvested by centrifugation (5,000 rpm) for 10 min at room temperature, and cell pellets were saponified at 80 °C for 2 h with 3 mL of MeOH, 2 mL of pyrogallol dissolved in MeOH (0.5%, *wt/v*) (CAS # 87-66-1, Sigma-Aldrich, St. Louis, MO.), and 2 mL of KOH (60%, *wt/v*). The non-saponifiable sterols were then extracted with 3×5 mL of heptane. The extracts were evaporated under a stream of nitrogen to dryness and resuspended in 500 µL of heptane. The sterol suspension was then transferred to a GC-MS vial and derivatized with 250 µL of *N*-methyl-*N*-(trimethylsilyl) trifluoroacetamide (MSTFA, CAS # 24589-78-4, Sigma-Aldrich, St. Louis, MO) at 70 °C for 20 min. GC-MS analyses were performed on an Agilent 7890A gas chromatograph with splitless injection, coupled to an Agilent 5970C inert XL mass spectrometer with a triple-axis detector and an Agilent 19091S-433 capillary column (30 m x 250 µm). The oven temperature was

programmed to hold at 70 °C for 2 min and then ramped to 270 °C at a rate of 20 °C/min. Helium (10 psi) was used as the carrier gas, the electron ionization energy was 70 eV, and the inlet temperature 250 °C. Identification of sterols was achieved using the NIST (the National Institute of Standards and Technology) reference database. These data are presented in Fig. 7.

3. References:

1. Clinical and Laboratory Standards Institute. Reference method for broth dilution antifungal susceptibility testing of yeasts - Approved standard. CLSI document M27-A3. Wayne, PA. **2008**.
2. Clinical and Laboratory Standards Institute. Reference method for broth dilution antifungal susceptibility testing of filamentous fungi - 2nd Edition: CLSI document M38-A2. Wayne, PA. **2008**.
3. Shrestha, S. K.; Fosso, M. Y.; Green, K. D.; Garneau-Tsodikova, S. Amphiphilic tobramycin analogues as antibacterial and antifungal agents. *Antimicrob. Agents Chemother.* **2015**, *59*, 4861-4869.
4. Fosso, M. Y.; Shrestha, S. K.; Green, K. D.; Garneau-Tsodikova, S. Synthesis and bioactivities of kanamycin B-derived cationic amphiphiles. *J. Med. Chem.* **2015**, *58*, 9124-9132.
5. Thamban Chandrika, N.; Shrestha, S. K.; Ngo, H. X.; Garneau-Tsodikova, S. Synthesis and investigation of novel benzimidazole derivatives as antifungal agents. *Bioorg. Med. Chem.* **2016**, *24*, 3680-3686.

4. Supplementary Figures (S1-S32):

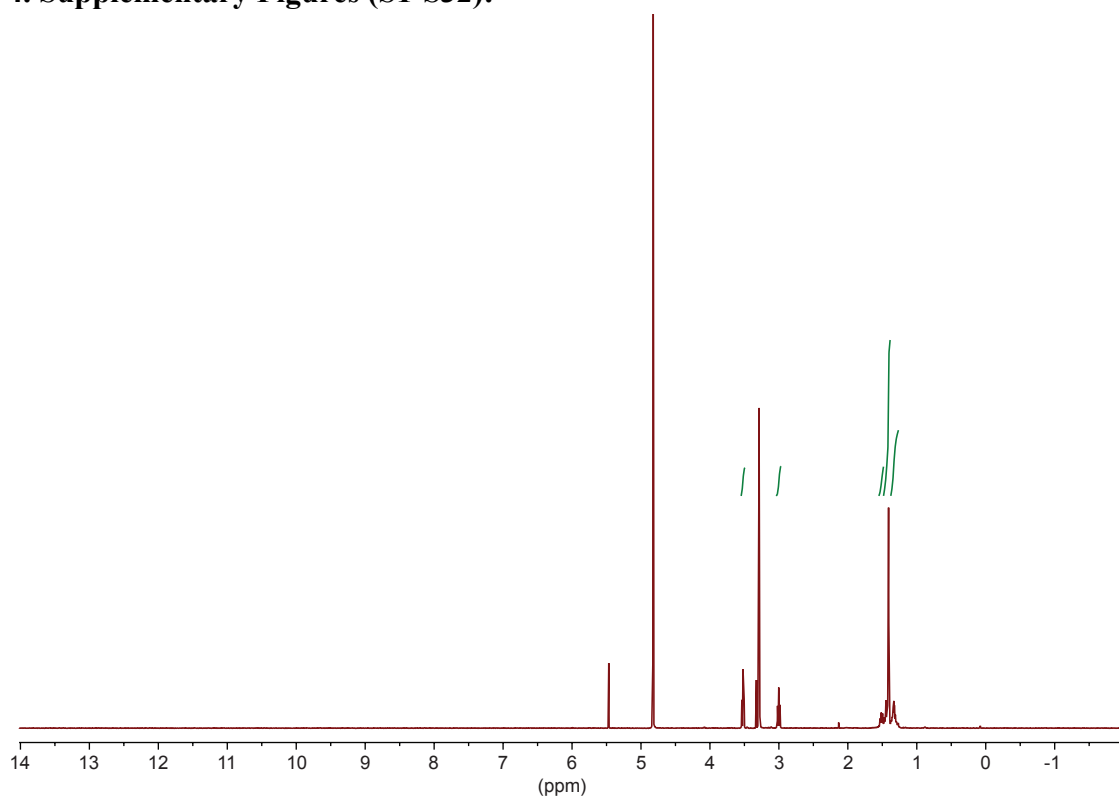


Fig. S1: ^1H NMR spectrum for compound **1** in CD_3OD (400 MHz).

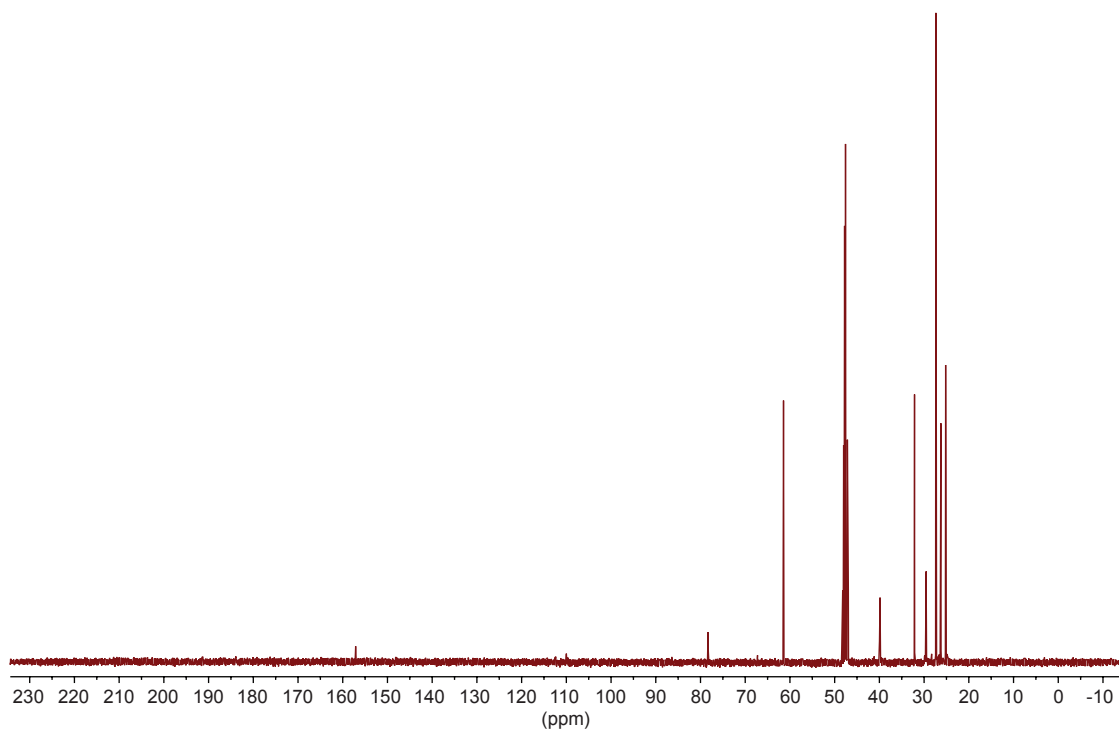


Fig. S2: ^{13}C NMR spectrum for compound **1** in CD_3OD (100 MHz).

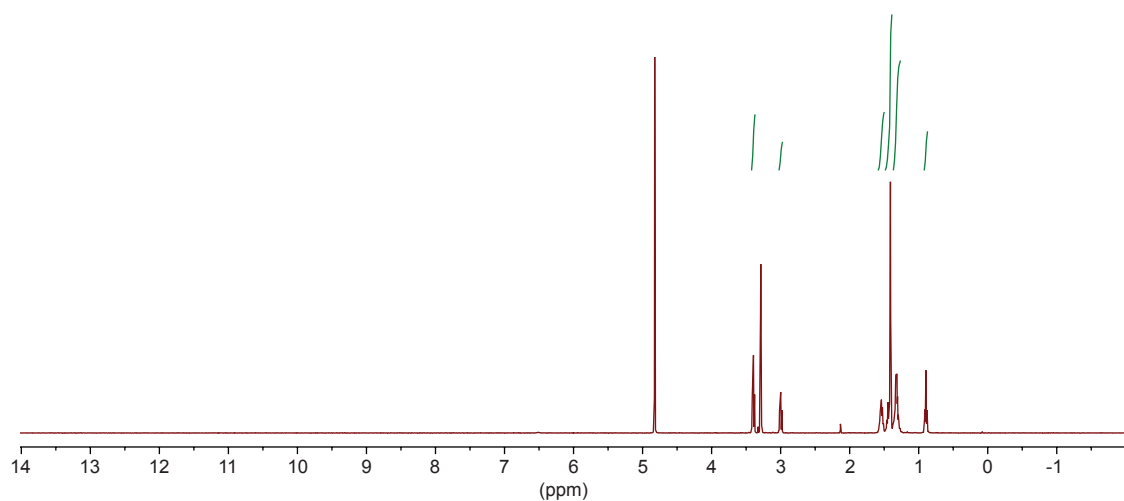


Fig. S3: ^1H NMR spectrum for compound **2** in CD_3OD (400 MHz).

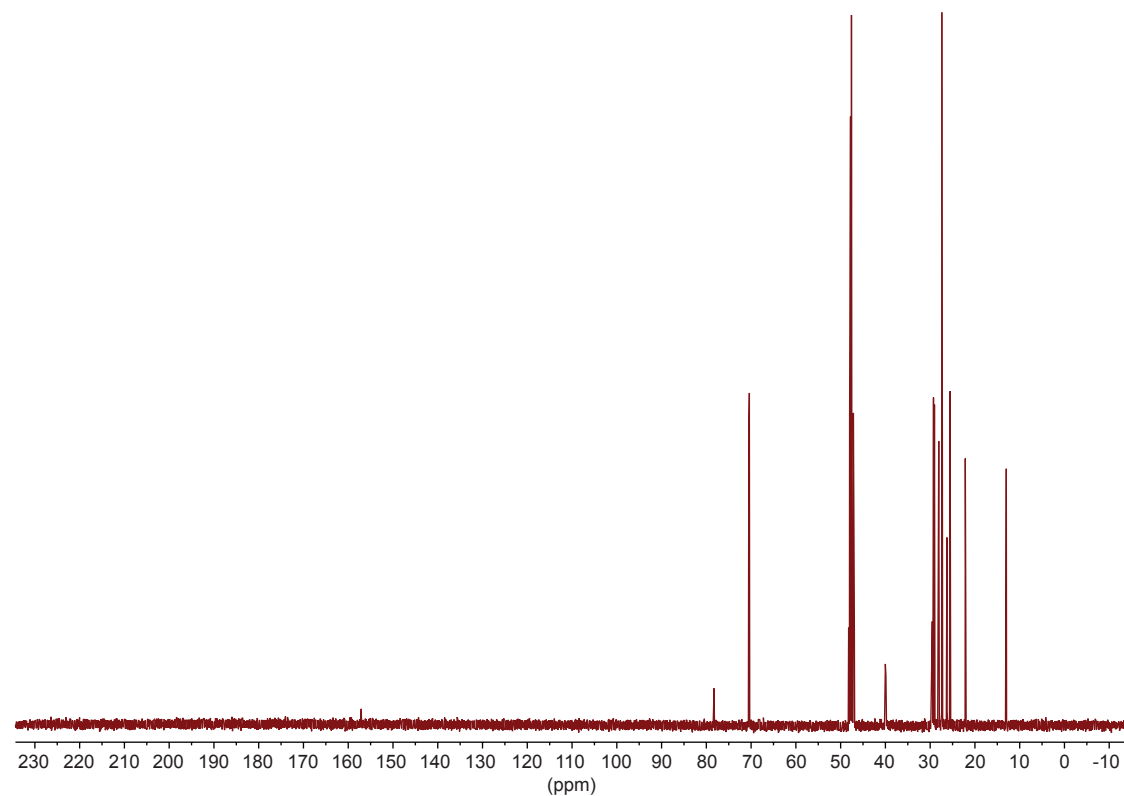


Fig. S4: ^{13}C NMR spectrum for compound **2** in CD_3OD (100 MHz).

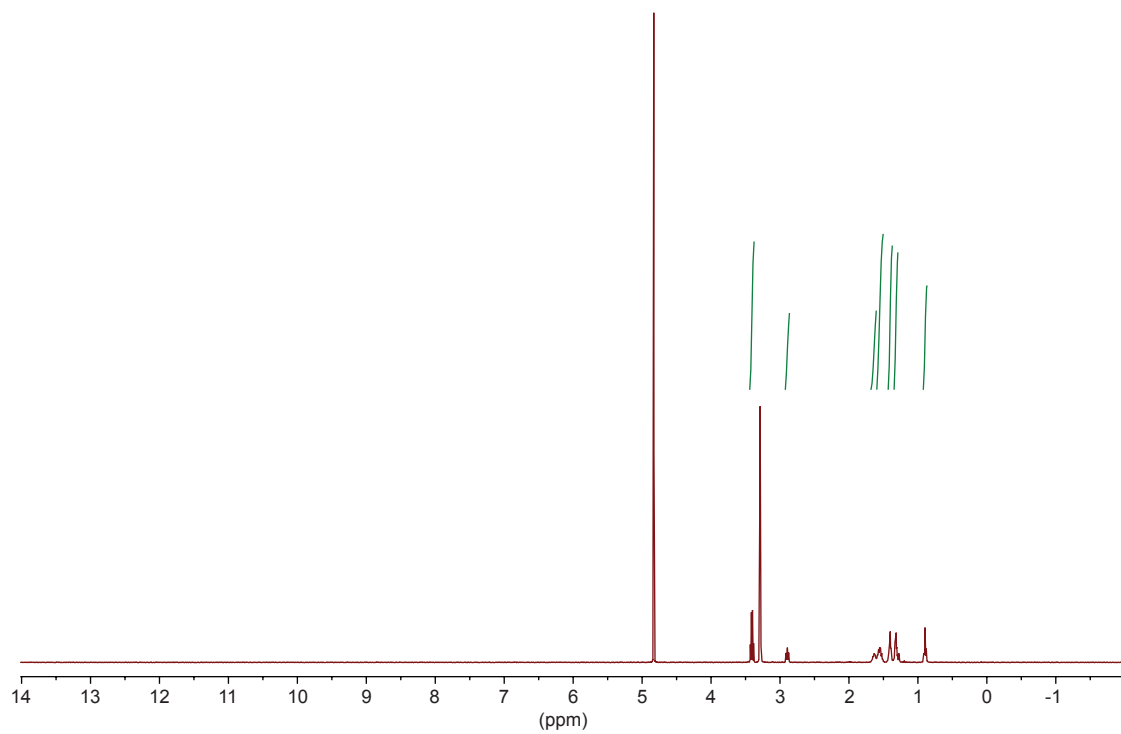


Fig. S5: ^1H NMR spectrum for compound **3** in CD_3OD (400 MHz).

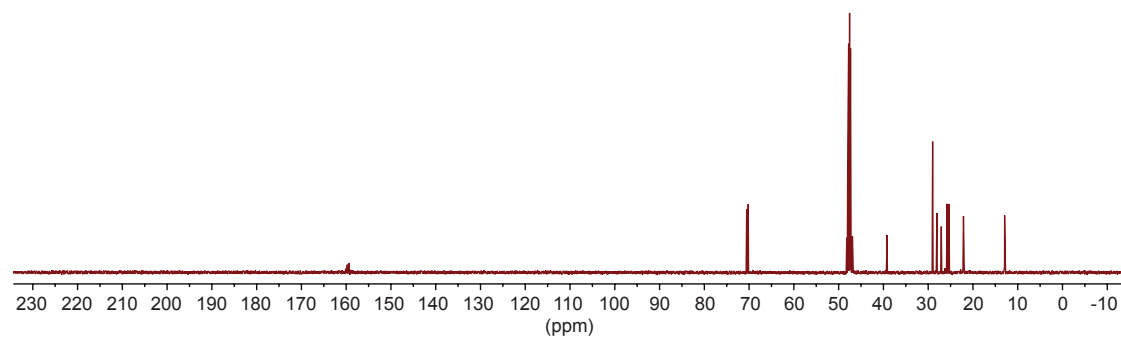


Fig. S6: ^{13}C NMR spectrum for compound **3** in CD_3OD (100 MHz).

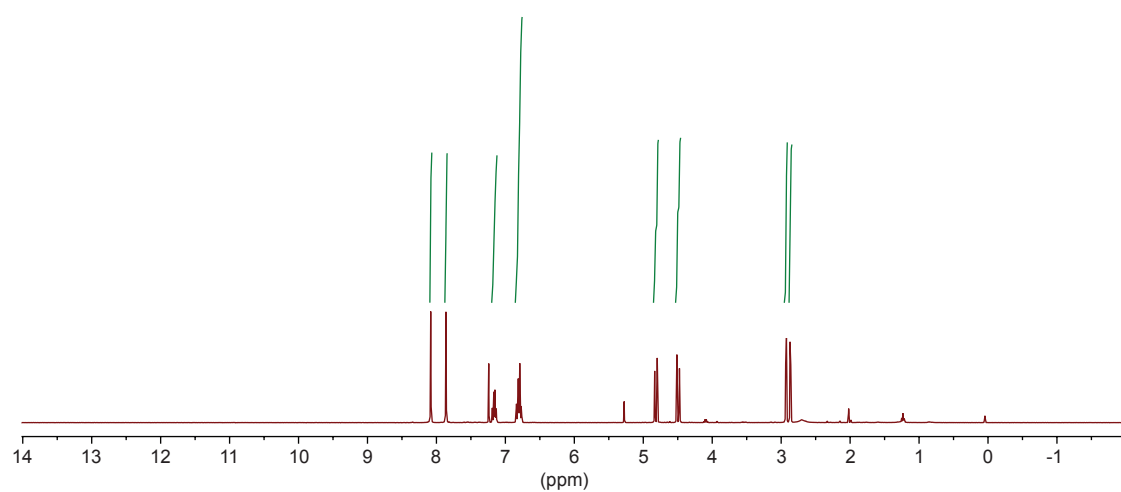


Fig. S7: ^1H NMR spectrum for compound **4** in CDCl_3 (400 MHz).

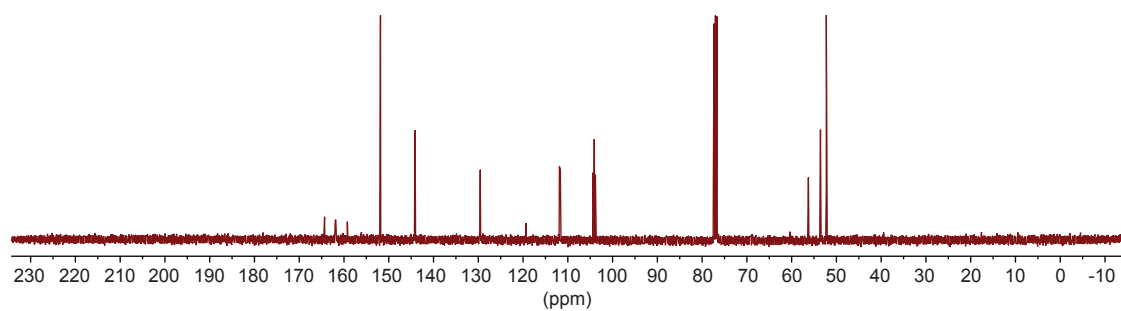


Fig. S8: ^{13}C NMR spectrum for compound **4** in CDCl_3 (100 MHz).

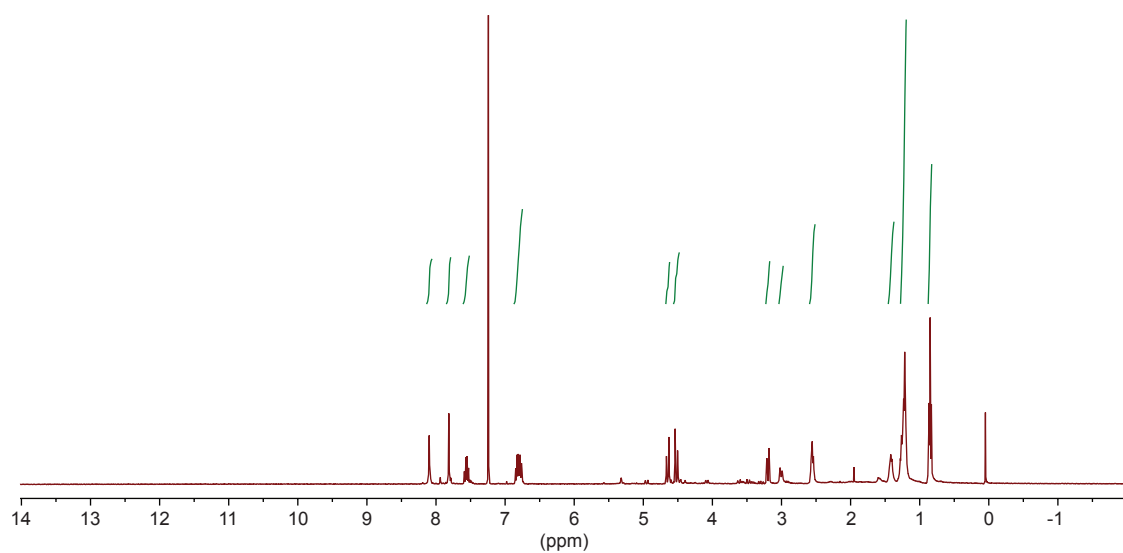


Fig. S9: ^1H NMR spectrum for compound **5** in CDCl_3 (400 MHz).

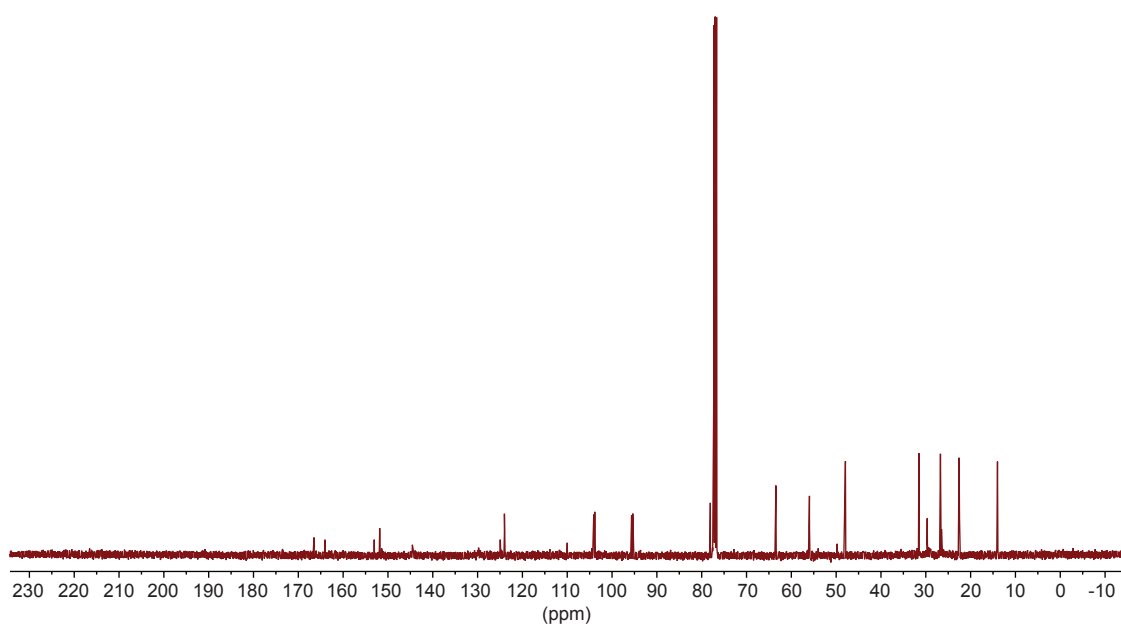


Fig. S10: ^{13}C NMR spectrum for compound **5** in CDCl_3 (100 MHz).

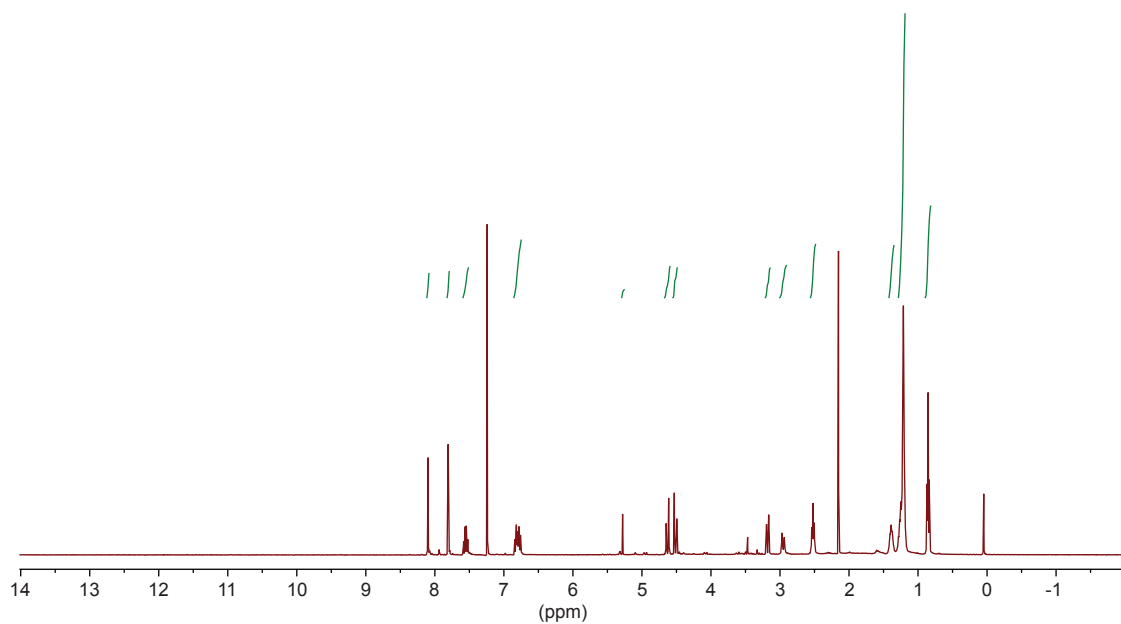


Fig. S11: ^1H NMR spectrum for compound **6** in CDCl_3 (400 MHz).

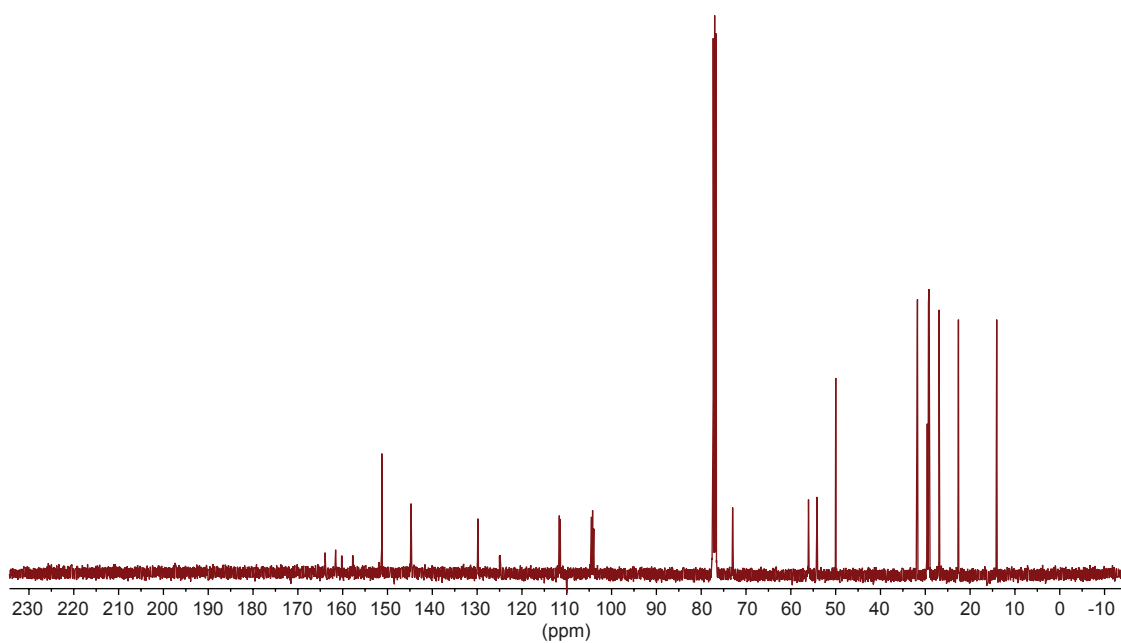


Fig. S12: ^{13}C NMR spectrum for compound **6** in CDCl_3 (100 MHz).

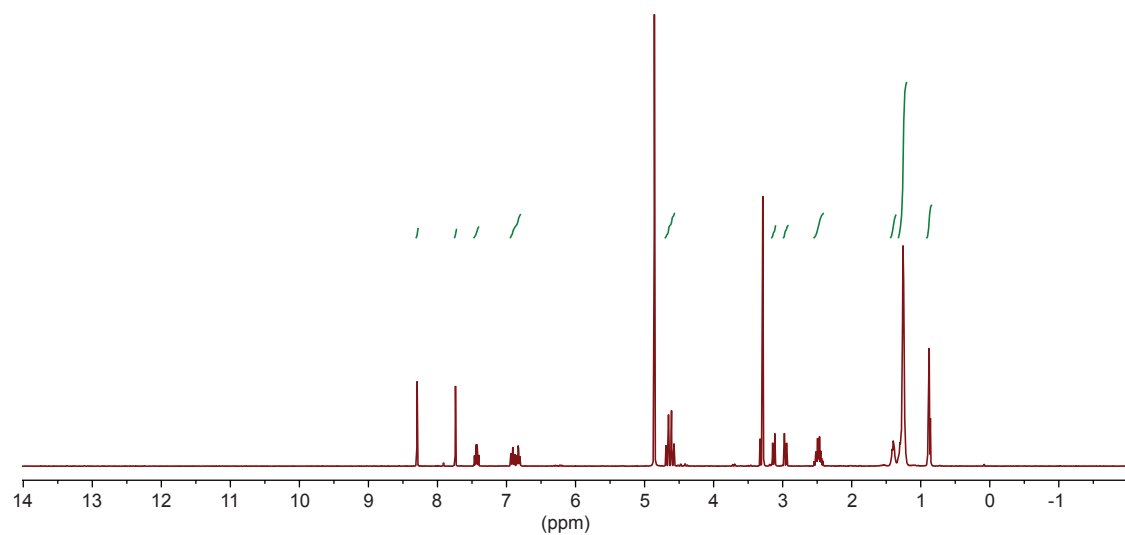


Fig. S13: ^1H NMR spectrum for compound **7** in CD_3OD (400 MHz).

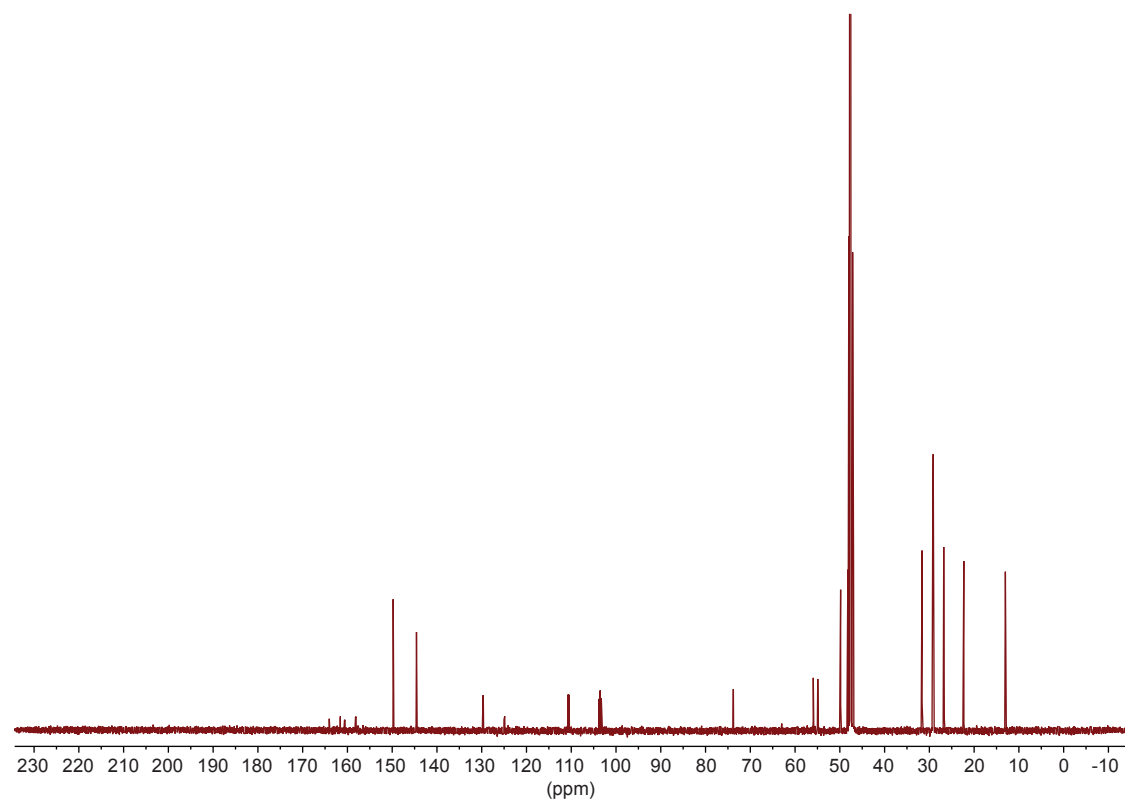


Fig. S14: ^{13}C NMR spectrum for compound **7** in CD_3OD (100 MHz).

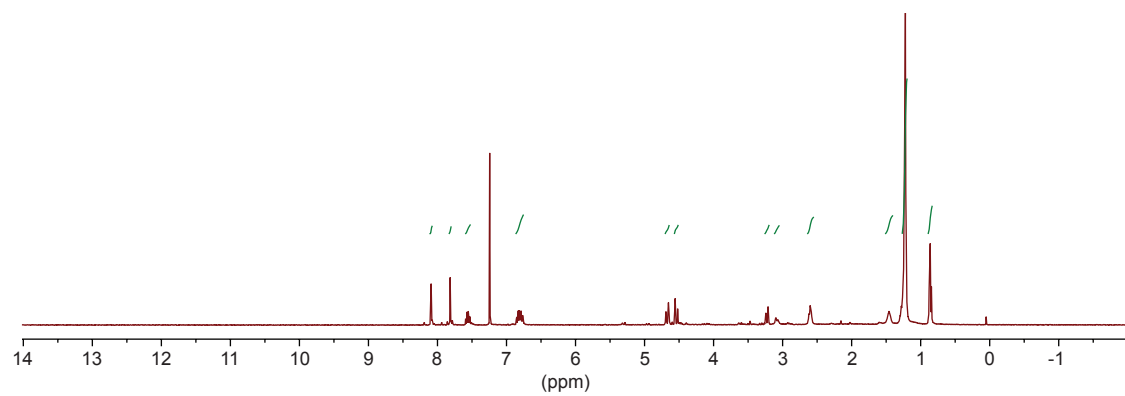


Fig. S15: ^1H NMR spectrum for compound **8** in CDCl_3 (400 MHz).

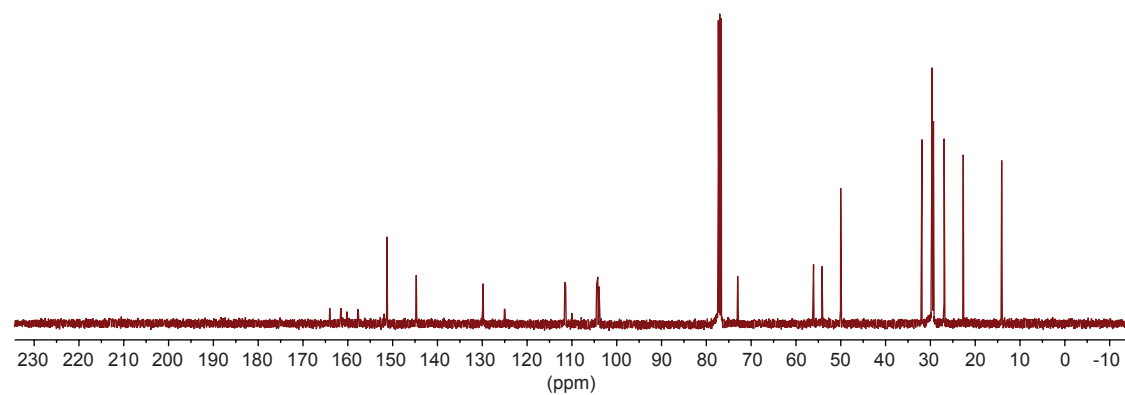


Fig. S16: ^{13}C NMR spectrum for compound **8** in CDCl_3 (100 MHz).

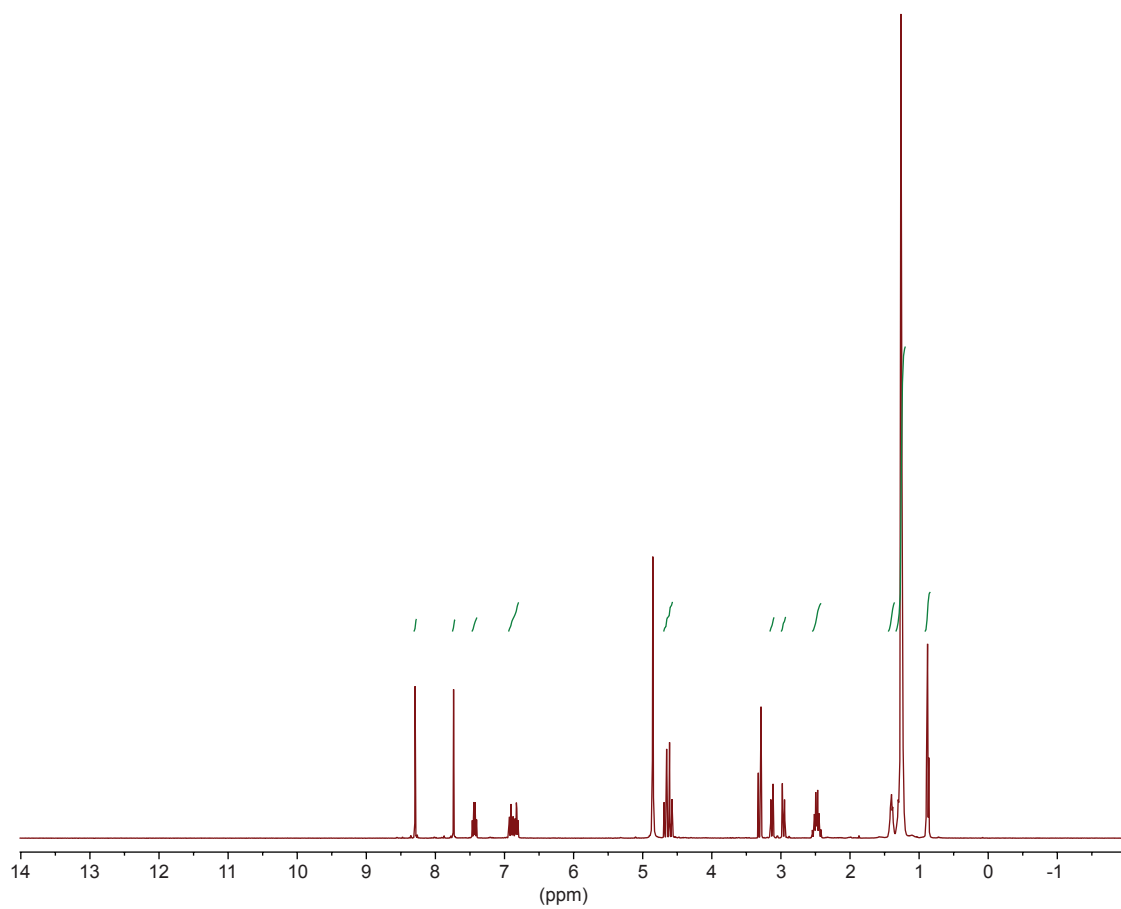


Fig. S17: ^1H NMR spectrum for compound **9** in CD_3OD (400 MHz).

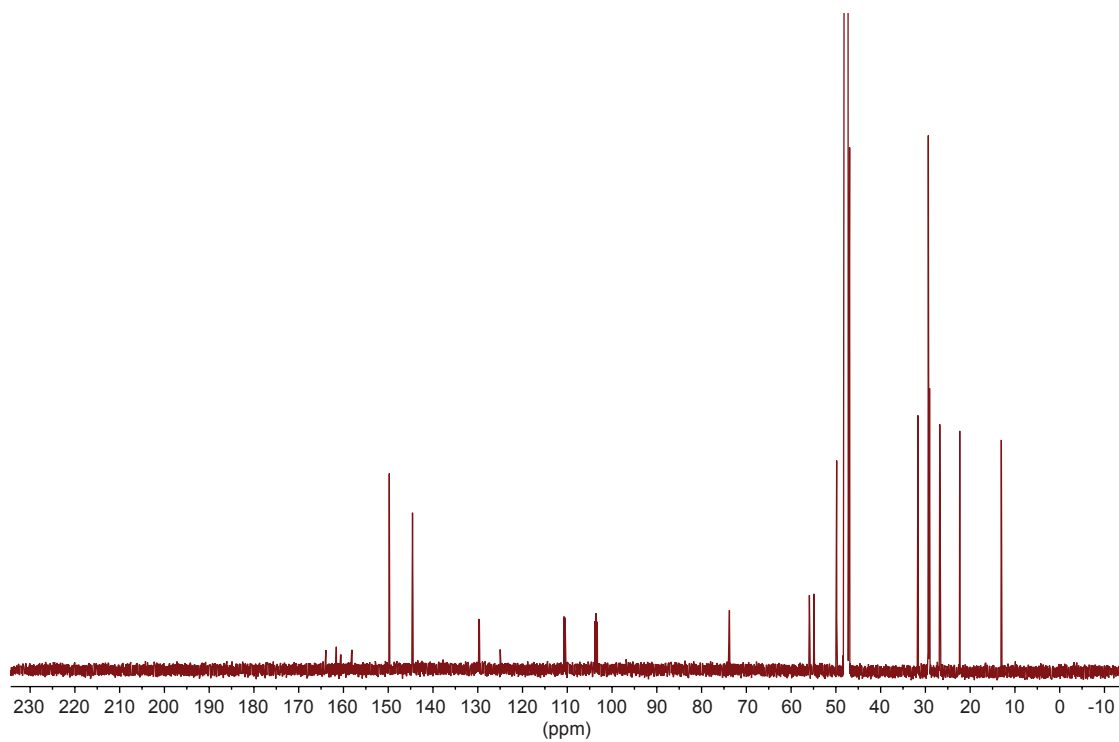


Fig. S18: ^{13}C NMR spectrum for compound **9** in CD_3OD (100 MHz).

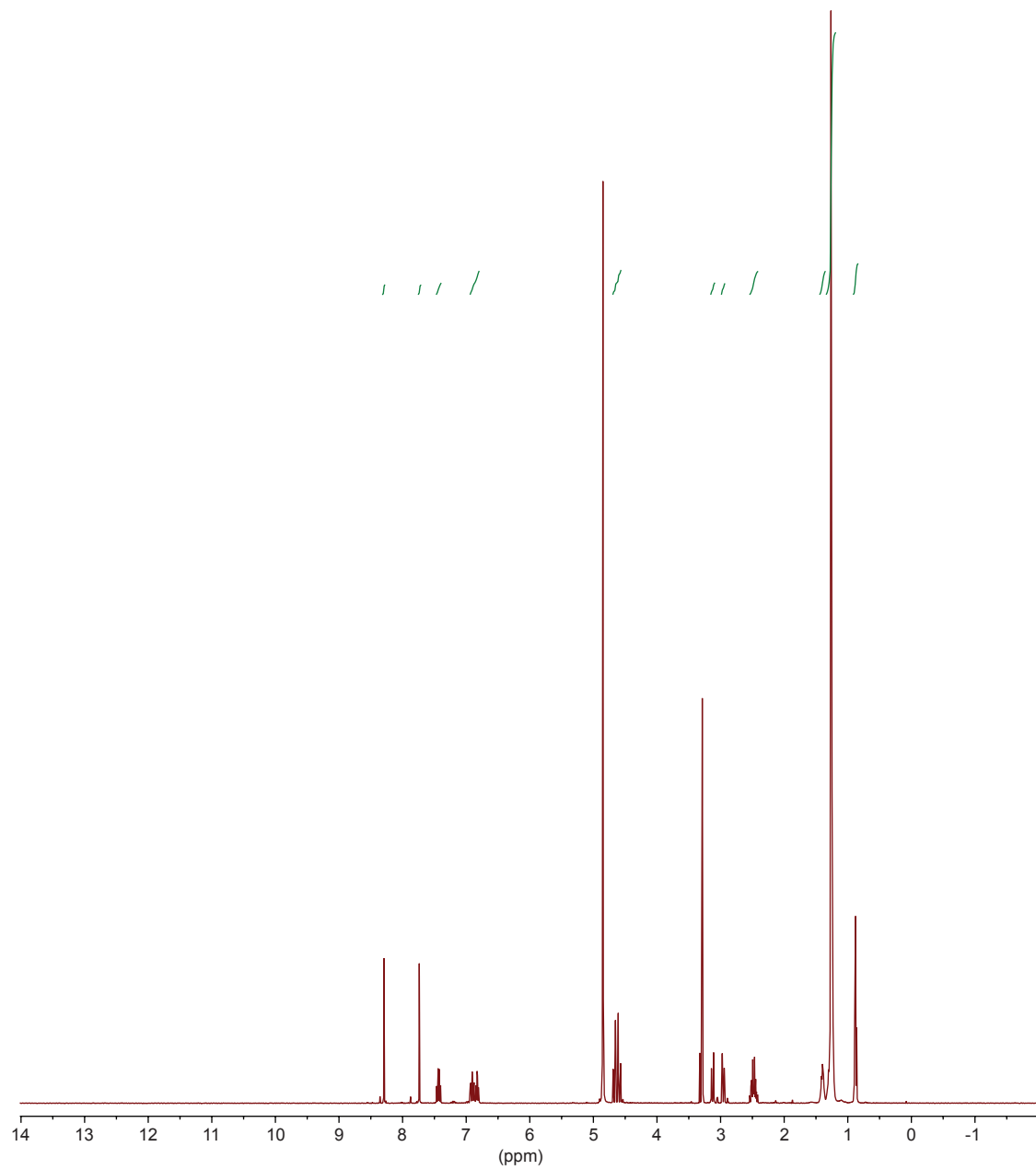


Fig. S19: ^1H NMR spectrum for compound **10** in CD_3OD (400 MHz).

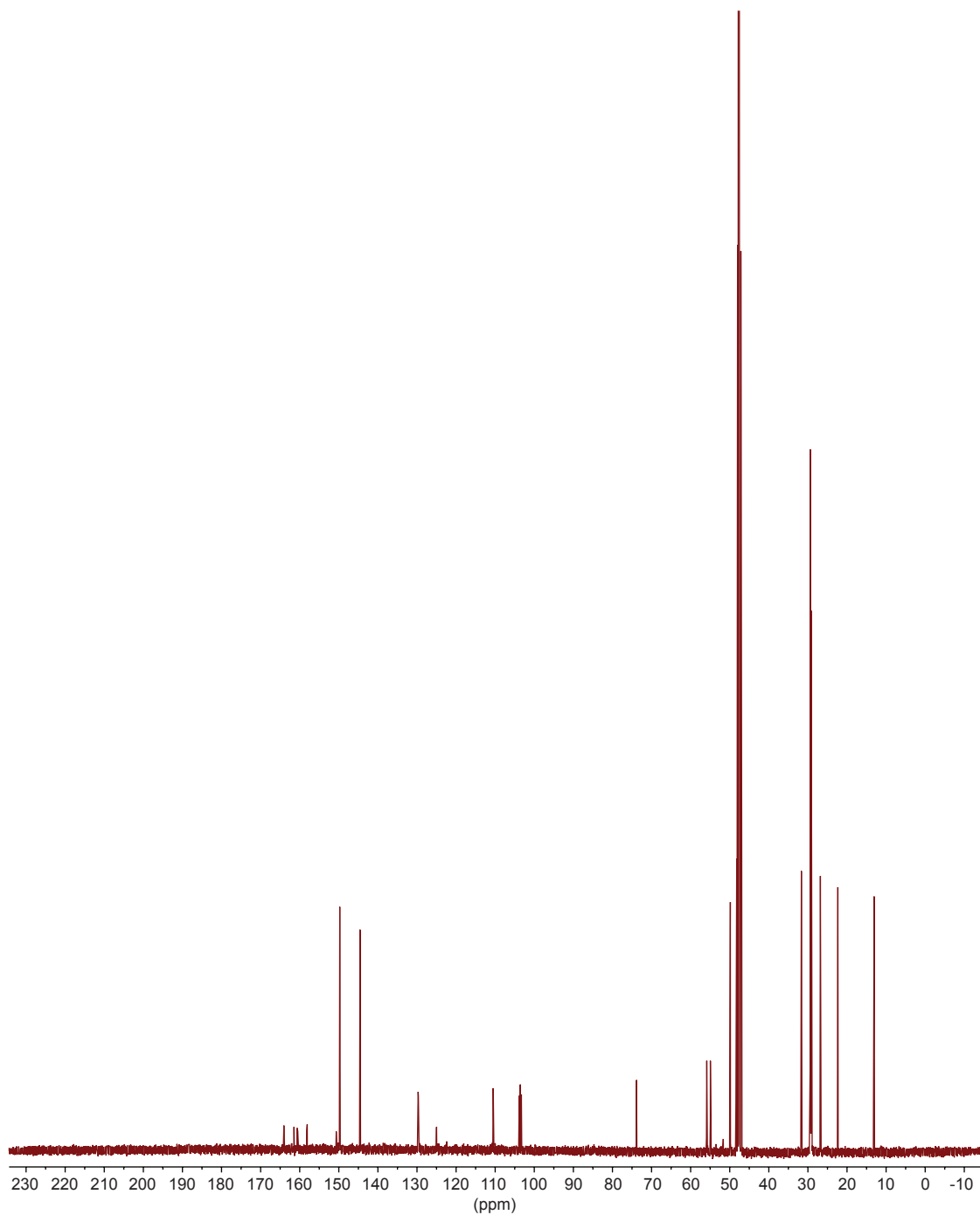


Fig. S20: ^{13}C NMR spectrum for compound **10** in CD_3OD (100 MHz).

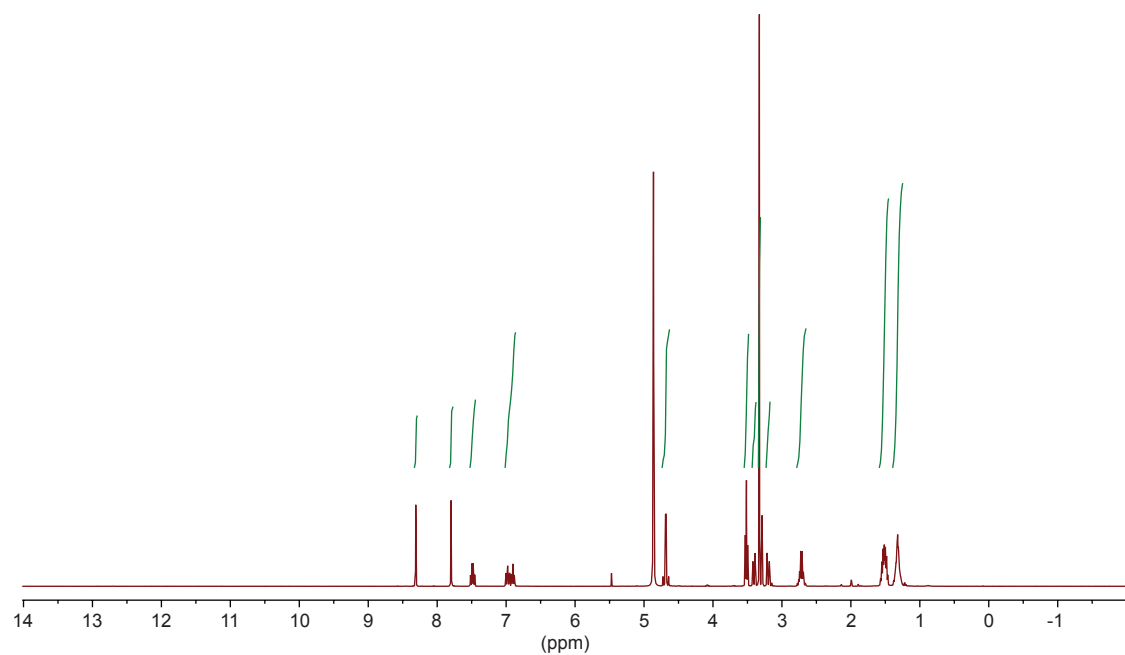


Fig. S21: ^1H NMR spectrum for compound **11** in CD_3OD (400 MHz).

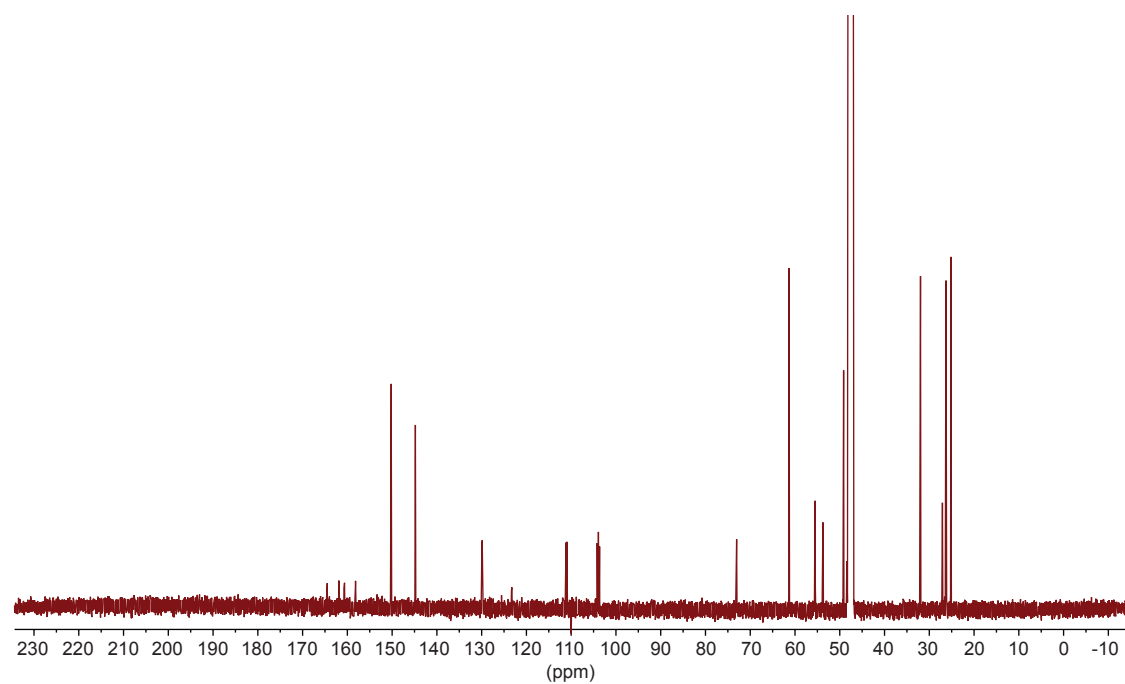


Fig. S22: ^{13}C NMR spectrum for compound **11** in CD_3OD (100 MHz).

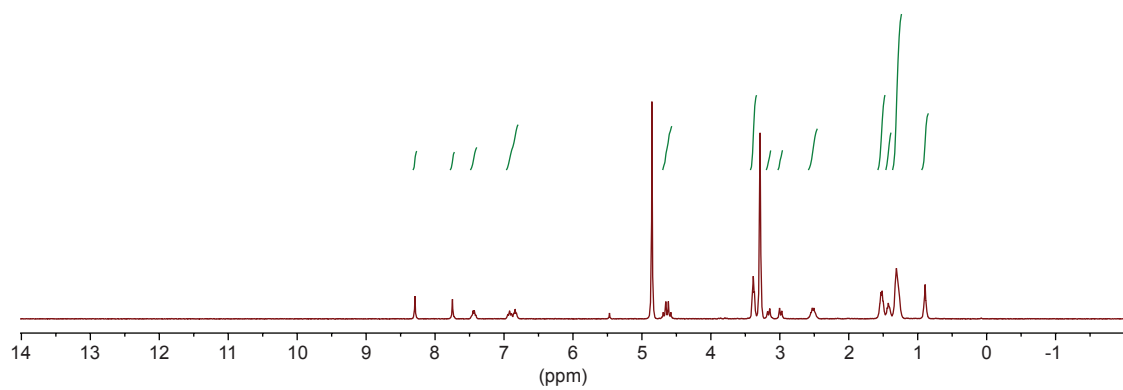


Fig. S23: ^1H NMR spectrum for compound **12** in CD_3OD (400 MHz).

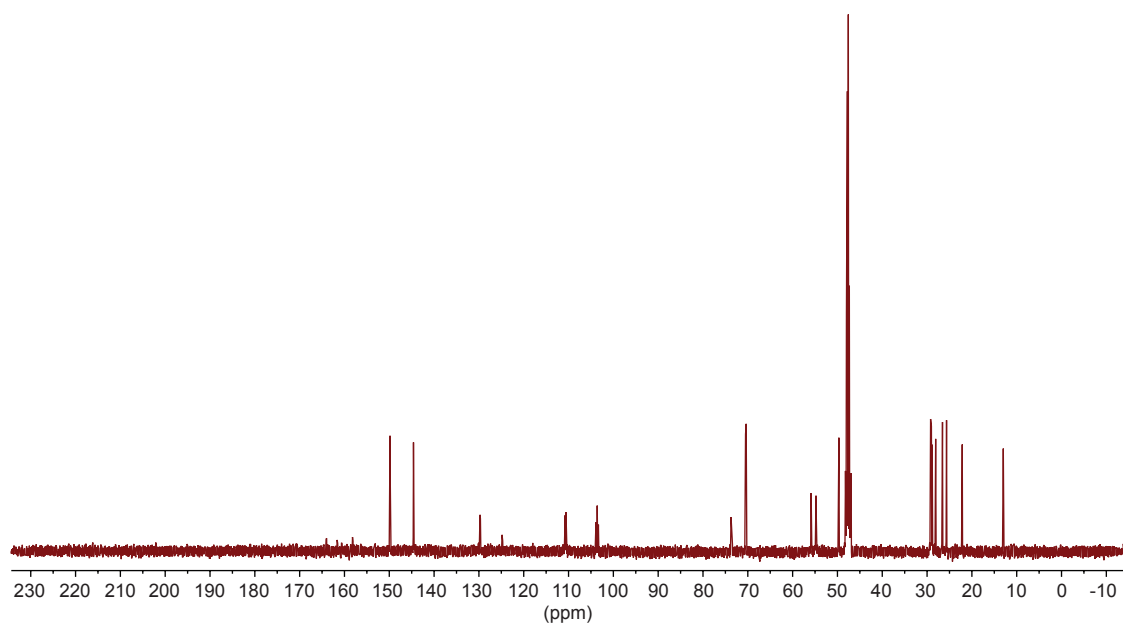


Fig. S24: ^{13}C NMR spectrum for compound **12** in CD_3OD (100 MHz).

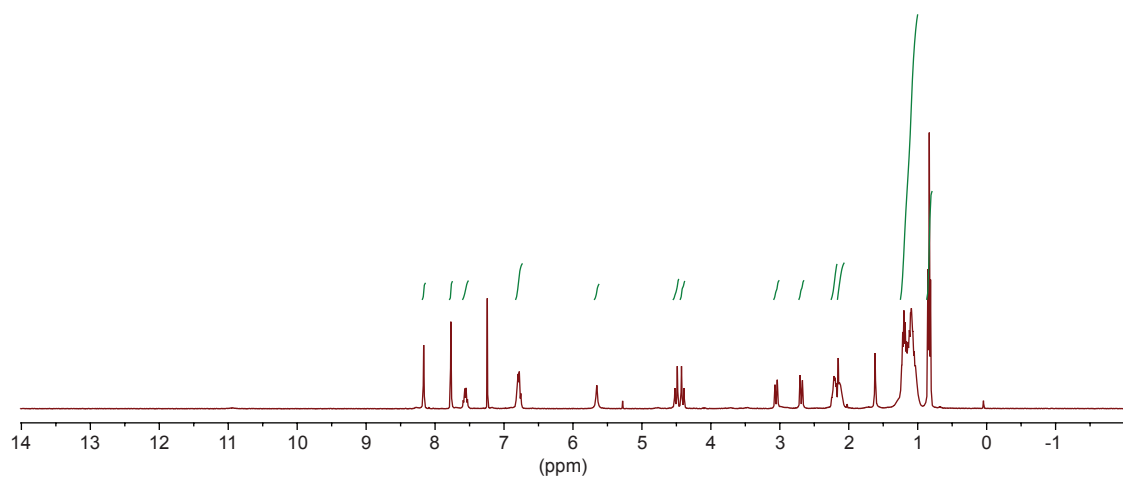


Fig. S25: ^1H NMR spectrum for compound **13** in CDCl_3 (400 MHz).

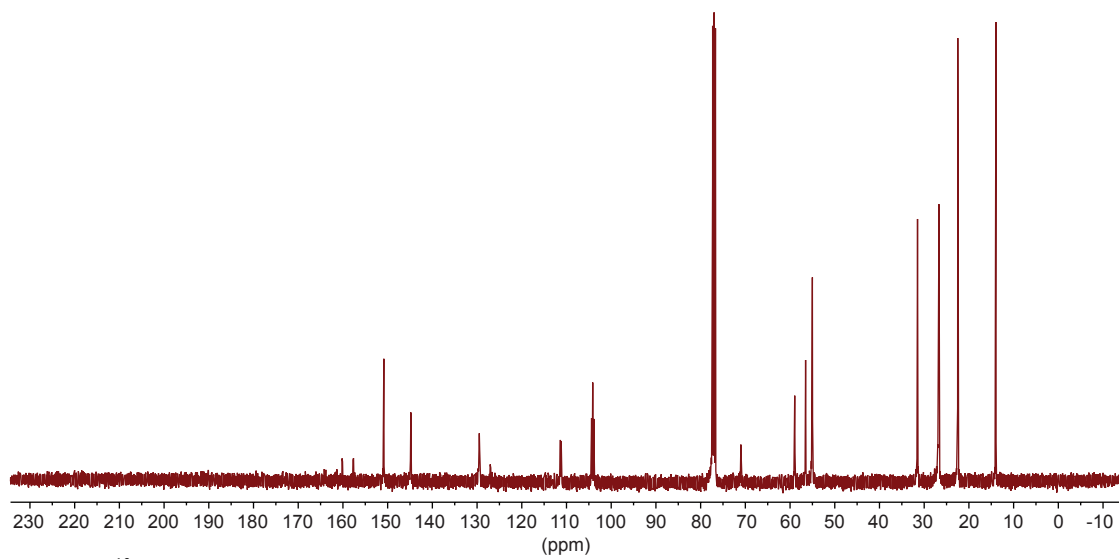


Fig. S26: ^{13}C NMR spectrum for compound **13** in CDCl_3 (100 MHz).

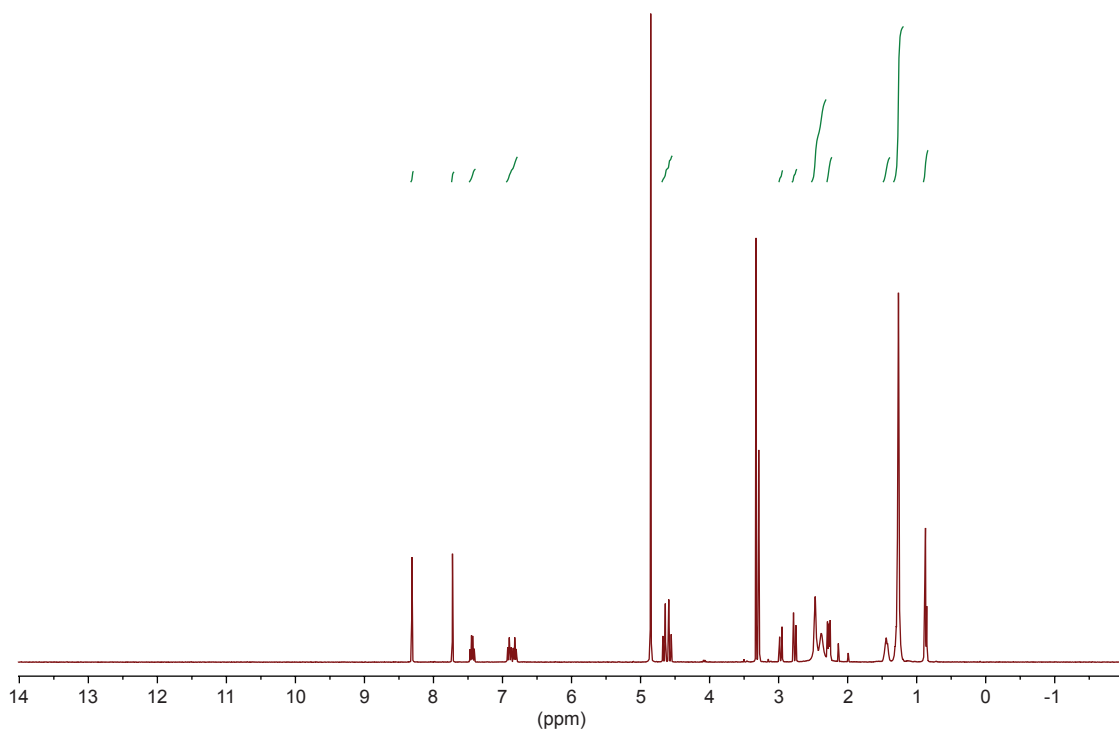


Fig. S27: ^1H NMR spectrum for compound **14** in CD_3OD (400 MHz).

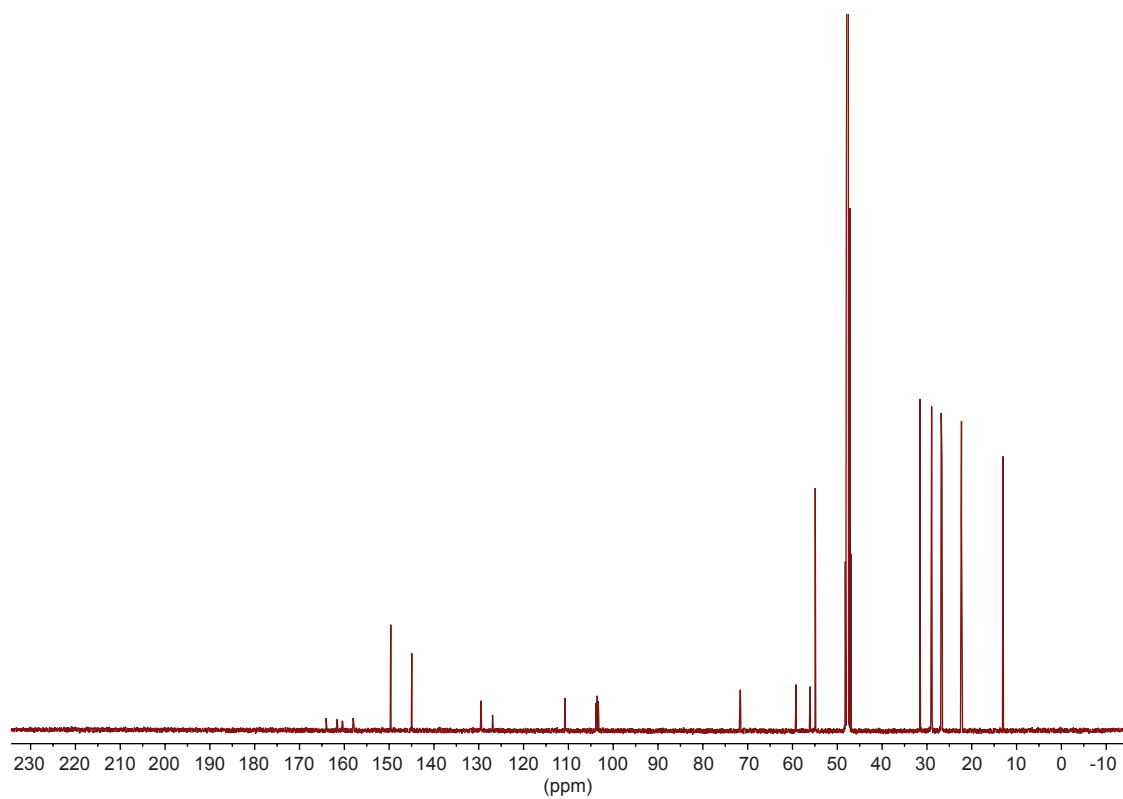


Fig. S28: ^{13}C NMR spectrum for compound **14** in CD_3OD (100 MHz).

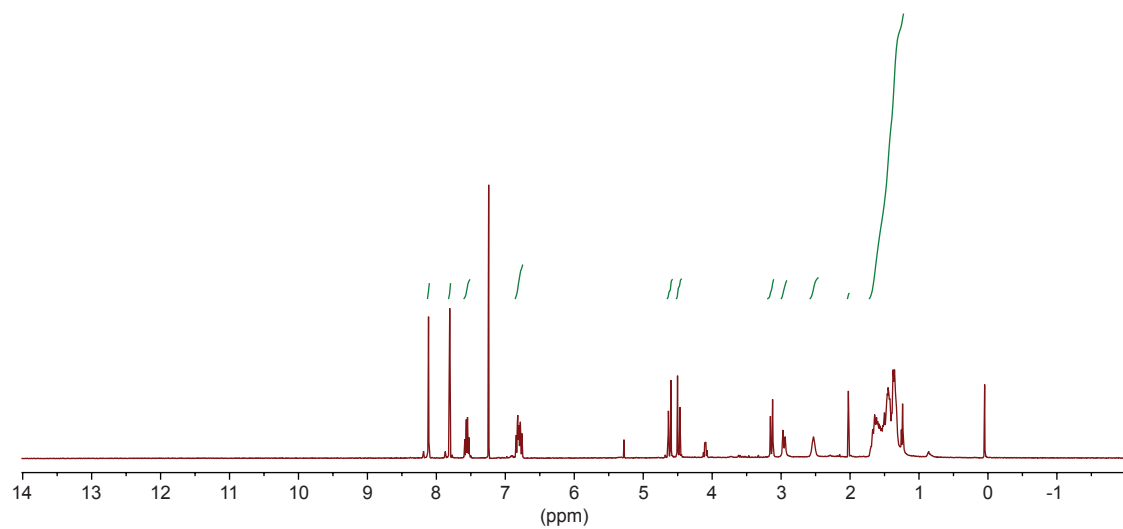


Fig. S29: ^1H NMR spectrum for compound **15** in CDCl_3 (400 MHz).

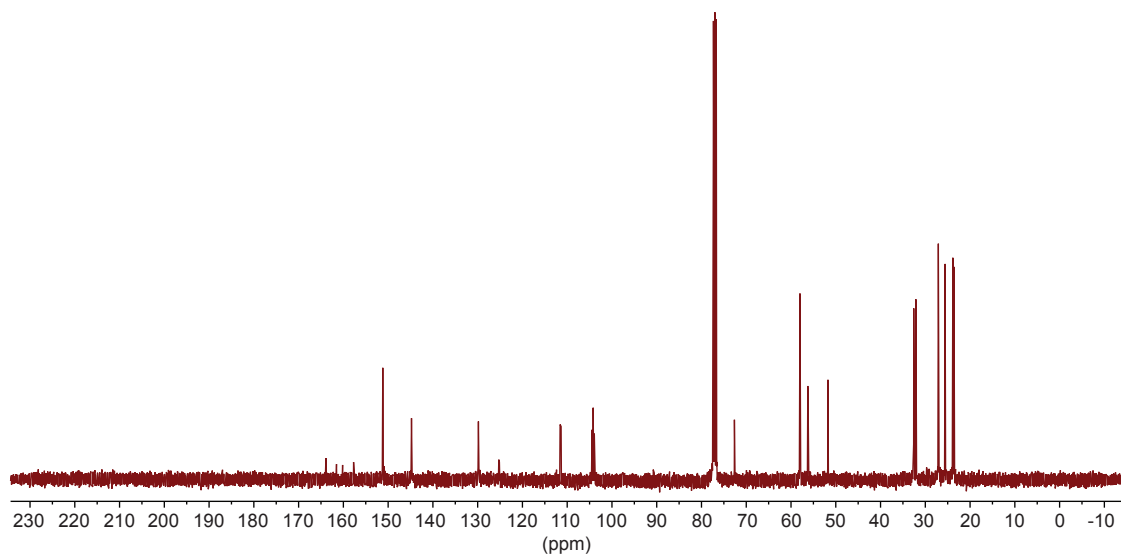


Fig. S30: ^{13}C NMR spectrum for compound **15** in CDCl_3 (100 MHz).

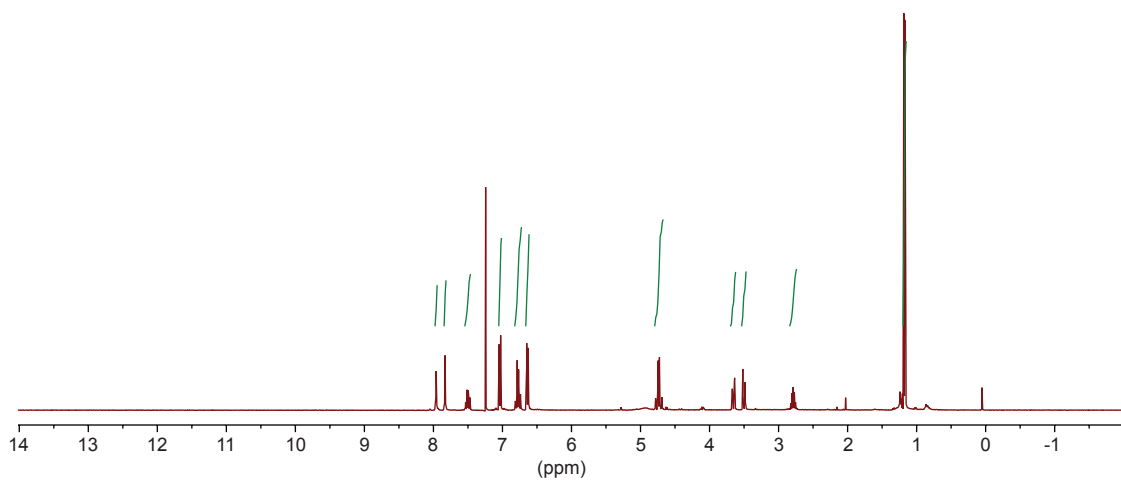


Fig. S31: ^1H NMR spectrum for compound **16** in CDCl_3 (400 MHz).

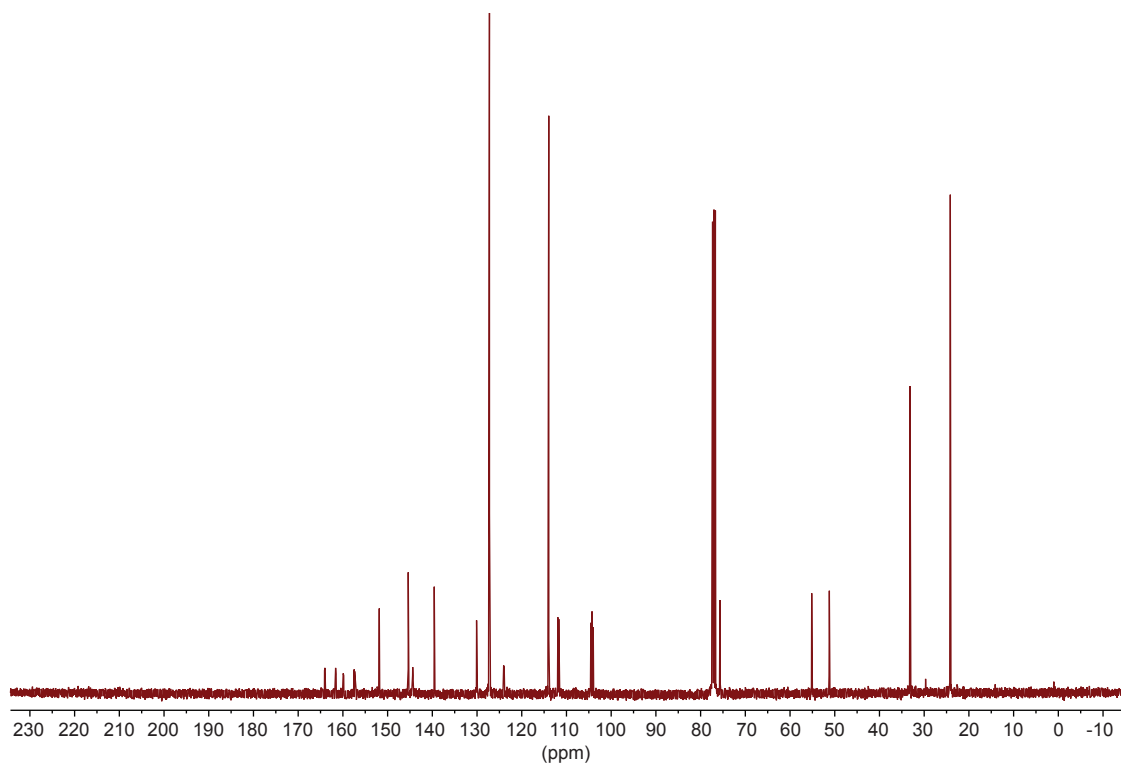


Fig. S32: ^{13}C NMR spectrum for compound **16** in CDCl_3 (100 MHz).